

## Response to Anonymous Referee #1:

We thank Anonymous Referee #1 very much for his/her helpful comments. Below are our point-by-point responses.

### 5 **Reviewer's comment [1]:**

Line 362-364: Because in section 2.2 only rough estimates are given for the size dependent sampling efficiencies of the different techniques, I recommend removing or weaken the statements about INP abundance in different size ranges here.

### 10 **Authors' response [1]:**

We propose to weaken the existing statements through appropriate wording, but retain a brief discussion that more clearly highlights the basis for the statements. We reference expected capture efficiencies of the filters in Section 2.2, and this should have been reiterated in this results section. These calculated capture efficiencies indicate that the 3-micron pore-size filters should be inefficient at capturing (on the surface or in pores) submicron diameter particles except those well below 0.1 microns in size, while the 0.2-micron pore-size filters have high efficiencies across all diameters. Since the INP concentration results are comparable on the two filter sizes, it suggests a size of INPs in the 1  $\mu\text{m}$  range or larger on average during these sampling periods.

### 20 **Changes in manuscript re: comment [1]:**

We rewrite,

*“Considering the capture efficiencies versus size noted in Section 2.2, the lack of significant difference in  $I_{S_{INPs}}$  measured with the filters of 0.2 and 3  $\mu\text{m}$  pore sizes implies that most INPs were likely large enough to be captured effectively. This crudely suggests an INP mode size at about 1  $\mu\text{m}$  or larger. This is also a size that is collected with high efficiency in the Biosampler, for which similar INP concentrations were measured.”*

### 25 **Reviewer's comment [2]:**

The black and blue crosses can hardly be distinguished in Figs. 1 and 2. I recommend using other colors or other symbols. Why are only 1:1 lines shown in Fig. 3? I recommend to also show linear fit lines to the data sets. Why are error bars only shown in panel d of Fig. 3?

### 30 **Authors' response [2]:**

We agree with the reviewer on most of these points. The black and blue crosses have been changed to triangles and a different distinguishing color (gold) is now used for the Biosampler in Figures 1 and 2. We have also added the requested error bars for all panels in Figure 3. The 1:1 line in Fig. 3 is shown as an expectation for perfect agreement. Since we spent two additional figures to discuss the discrepancies between methods as a function of temperature, which in some cases is not linear, we resisted showing linear fit lines in the panels of Fig. 3. The reasoning initially was manifold. First, although these would show a general trend, the fit itself would not add any valuable information on exactly what is going on. The 1:1 line is also the basis for extrapolating perfect agreement on assuming that the CFDC instrument underestimates all natural INPs by the factor that has been reported for mineral dust particles in the laboratory and field. Finally, we spent a great deal of effort in the paper to explain that perfect overlap of samples was a difficult task that requires a lot coordination (and expense on the part of volunteering groups), with the consequence that only a small amount of data amenable to something like statistical tests was acquitted. When showing data without perfect overlap, the discussion should be a bit more general, as we provide in Fig. 4 and Fig. 5. Nevertheless, since both reviewers have requested these fits, we place them now in addition to the existing lines.

### 45 **Changes in manuscript re: comment [2]:**

The new figures appear at the end of this response, as they will be shown in the final article. At the point of introducing these fits in section 3.2 we write:

*“The linear relational slope between  $I_S$  and CFDC data shown by the light gray dashed line in Fig. 3a. The same representation is applied in all panels of Fig. 3. We provide these fits only to show general trends between the different data sets and do not provide fit parameters herein because a deeper consideration of the source of discrepancies requires additional inspection of trends as a function of temperature, which follows below.”*

**Reviewer’s comment [3]:**

Conclusions line 540: I would not say the agreement achieved is excellent. In my view it is good or very good within uncertainty limits.

60

**Authors’ response [3]:**

We agree with the reviewer.

**Changes in manuscript re: comment [3]:**

65 We have modified the sentence accordingly as, “Very good agreement within uncertainty limits was obtained under...”

**Response to Anonymous Referee #2:**

70

We thank Anonymous Referee #2 for his/her careful comments that help to improve our presentation. Below are our point-by-point responses.

**Reviewer’s general comment [1]:**

75 One difficult aspect of digesting the submitted work is that it is at times unclear what instrument specific discussion points can be found in the cited papers (generally dedicated to individual instrument systems) and what is more specific to what is presented in this manuscript. Although, I expect many interested readers have also read the cited literature it is difficult to keep it all at the forefront of one’s thoughts. Thus, I would suggest that in revision the authors attempt to more clearly enumerate where instrument specific information can be found in referenced  
80 literature and where they are making new statements. For example, the issue of sample storage is raised multiple times but addressed in different ways – it is a challenge to repeatedly return to the literature to see how different instrumental systems have responded to (or not responded to) sample storage and what if any error this introduces.

**Authors’ general response [1]:**

85 We appreciate the reviewer’s comment and believe that we understand how to fix this, at least in the case noted (storage of samples). However, we are not sure what other specific information is not present that one would need to reference. We acknowledge some difficulty in deciding how to introduce the methods, various comparisons done at different sites, when there was sampling sharing, and so forth. Hence, we decided to introduce the instrumental method first (including how processing of samples occurs and how calculations are made), then special collection  
90 considerations, and then the sample sites and objectives in each case. In settling on an approach to organizing this section of the paper, a few things were left a little scattered, and sample storage protocol was one of these. To fix this issue, we have consolidated the discussion of all storage protocol to the same section (Section 2.2). This primarily involved moving the statements about how the UBC group stored their samples. For CSU, NCSU, and NIPR, samples were either collected together and stored frozen always, or frozen in the same manner (excepting -20  
95 versus -80°C at times) by all groups, whether that be a filter or Biosampler sample. It should be understood that similar storage protocol or any issues with storage were not things fully-considered at the start of common sampling that then extended over a few years’ time. We were not seeking to recommend protocol but to represent how different groups treat storage.

100 As discussed by Petters and Wright (2015) in their study of INP measurements from rainwater, the argument that INP activity remains unaltered by the freezing of samples and subsequent storage for some time is at the core of use of immersion freezing methods. They noted the generally better than 1°C repeatability of median population freezing temperatures for droplet suspensions that undergo repeated freeze/thaw cycles [Vali, 2008; Wright et al., 2013, and references therein] in support of their argument. We therefore reference  
105 Petters and Wright (2015) and references therein here, and we qualify our statement that our own investigations of this issue indicating (negligible, but not stated here) effects will be covered in a forthcoming paper that can include the type of statistical statement the reviewer would prefer to see. We have added words regarding thawing of samples, and on assumptions that, for the most part, storage impacts should have been the same, and that this is an additional topic for consideration in future comparisons due to the possibilities of particularly sensitive INPs.

110

**Changes in manuscript, re: general comment [1]:**

We now write in Section 2.2.:

115 “After particle collection, filters were stored frozen at -25 or -80°C in sealed, sterile petri dishes until they could be processed (few hours to few months). Biosampler samples were similarly stored frozen and processed over similar time frames. MOUDI collections for the DFT method were vacuum-sealed after collection, stored at 4°C in a refrigerator, shipping was done with cold packs prior to cold-stage flow cell measurements at the University of British Columbia. We therefore assume similar impacts, if any, of storage on INPs following thawing for processing. This study was not initially conceived as one to test storage impacts on INPs, which should be addressed in future research. We do not expect storage methods to impact result on the basis of existing documentation in the literature.

120 For example, in their study of INPs in rainwater, Petters and Wright (2015) noted that the argument that INP activity remains unaltered by the freezing of samples and subsequent storage for some time is at the core of the general application of immersion freezing methods. They noted, with reference to other literature, the generally better than 1°C repeatability of freezing temperatures for droplets that undergo repeated freeze/thaw cycles.”

125 In the Conclusions, at the end of paragraph two, we now write:

“The assumed negligible effect of exact sample storage conditions and the timing of processing after thawing from frozen conditions on INP activity should be inspected more carefully in the future, since some INPs may be susceptible to thermodynamic cycling.”

130 **Reviewer’s general comment [2]:**

For some such issues tables, for example including the instrument specific sampling and temperature uncertainties or tolerances, in the text or supplementary material may be beneficial.

135 **Authors’ general response [2]:**

The reviewer notes some important absent information. We were in fact counting on readers accessing other recent papers that include many of these methods, and statements therein regarding uncertainty and precision that groups attempt to apply uniformly in their work. Our preference now is to insert a synopsis of this information directly into the manuscript under each instrument, and reference to previous publications that include this information. The sections describing each instrument will include some additional details, and we will introduce uncertainty calculations within each section. In all cases, these have remained consistent with what is published.

140

**Changes in manuscript, re: general comment [2]:**

145 In the description for the CS we add: “Temperature uncertainty is based on the manufacturer’s (Model TR141-170, Oven Industries) stated tolerance of the cold plate thermistor ( $\pm 1^\circ\text{C}$ ).” Regarding confidence intervals, we write, “Analysis of CS repeat trial data involved binning data into 1°C intervals. Confidence intervals were calculated using two standard deviations of the geometric mean for each bin where multiple data points were available.”

150 For the IS we add: “Temperature was measured with 0.1°C resolution and 0.4°C accuracy (Hill et al., 2016)” For confidence intervals, “Binomial sampling confidence intervals (95%) were determined for IS data, as described in Hill et al. (2016).”

The description of MOUDI calculations has been revised as discussed in response to the next comment. We also add, “Confidence intervals (95%) were calculated based on the Poisson distribution, following Koop et al. (1997). These intervals are nearly equivalent to Binomial confidence intervals for the data in this study.”

155

For the CRAFT instrument, we add, “Binomial confidence intervals (95%) were determined, as for the IS data.”

For the CFDC we write, “CFDC measurement uncertainties vary with processing conditions, and are typically  $\pm 0.5^\circ\text{C}$  and 2.4% water relative humidity at  $-30^\circ\text{C}$  (DeMott et al., 2015).”

160 Separately, we write,

“We follow Schill et al. (2016) for correcting sample concentrations for background and for defining confidence intervals for CFDC data, which are represented by error bars in presented plots. Specifically, correct INP concentrations are the sample concentrations with the interpolated background concentrations subtracted. The standard deviation derived from the Poisson counting error during both the sample and the interpolated background concentrations were added in quadrature to obtain the INP concentration error. Concentrations are considered significant if they are 1.64 times larger than the INP concentration error, which corresponds to the Z statistic at 95% confidence for a one-tailed distribution. Consequently, although the lowest limit of detection for 10-min sampling intervals is  $\sim 0.2 \text{ L}^{-1}$ , significant data often requires in excess of  $1 \text{ L}^{-1}$  INP concentrations.”

165

170 We have accordingly revised and tightened up the remaining discussion in Section 2.1 regarding CFDC uncertainties and relation to using the aerosol concentrator.

**Reviewer's minor comment [1]:**

175 lines 215-220:  $f_{nu}$  and  $f_{ne}$  must be explicitly defined. In the cited literature  $f_{nu}$  exists for 2 size ranges and it is unclear what is referred to here. Possibly a combination of the two? Furthermore, at least a sentence or two should be dedicated to an explanation of the origin of these correction factors. This is where the link to the cited material should be provided. Also, please make clear if the parameters used are identical to those previously published, or are they specific to the particular sample analysis? A short reading of the two papers does not make this evident.

180 **Authors' response to comment [1]:**

We appreciate the reviewer's pointing out this need to go beyond our simplified explanation.

**Changes in manuscript re: comment [1]:**

185 To address this comment, we have expanded considerably the description of the correction factors and error analysis associated with the MOUDI-DFT technique. Tables are also added to the supplemental section so that correction factors are explicitly listed. We have revised the previous text listed below:

190 *"where  $N$  is the total number of droplets condensed onto the sample in this case,  $A_{deposit}$  is the total area of the sample deposit on the hydrophobic glass cover slip,  $A_{DFT}$  is the area of the sample monitored in the digital video during the droplet freezing experiment,  $V$  is the volume of air sampled by the MOUDI,  $f_{ne}$  is a correction factor to account for the uncertainty associated with the number of nucleation events in each experiment, and  $f_{nu}$  is a correction factor to account for non-uniformity in particle concentration across each MOUDI sample (Mason et al., 2015; Mason et al., 2016)."*

195 This section has been changed to read:

200 *"where  $N$  is the total number of droplets condensed onto the sample in this case,  $A_{deposit}$  is the total area of the sample deposit on the hydrophobic glass cover slip,  $A_{DFT}$  is the area of the sample monitored in the digital video during the droplet freezing experiment,  $V$  is the volume of air sampled by the MOUDI.  $f_{ne}$  is a correction factor to account for the statistical uncertainty that results when only a limited number of nucleation events are observed.  $f_{ne}$  was calculated following the approach given in Koop et al., (1997) using a 95% confidence interval.  $f_{nu}$  is a correction factor to account for non-uniformity in particle concentration across each MOUDI sample (Mason et al., 2015; Mason et al., 2016). This later correction factor consists of two multiplicative terms:  $f_{nu,1mm}$  and  $f_{nu,0.25-0.10 mm}$ , with these terms correcting for non-uniformity in the particle deposits at the 1mm and 0.25-0.1 mm scale, respectively. Since only a small area ( $1.2 \text{ mm}^2$ ) of the particle deposits are analyzed and the concentration of particles are not uniform across the entire substrate,  $f_{nu,1mm}$  needs to be applied. Since the concentration of particles are not uniform within the small area of the particle deposits analyzed for freezing,  $f_{nu,0.25-0.10 mm}$  needs to be applied. Listed in Tables S3 and S4 are the  $f_{nu,1mm}$  and  $f_{nu,0.25-0.10mm}$  values applied to the MOUDI-DFT samples collected at CSU and Kansas, respectively. Different correction factors were used for the CSU and Kansas samples since different substrate holders were used to position the glass slides within the MOUDI at the two sites. Substrate holders were not yet employed during the earlier MEFO studies (Huffman et al., 2013). However, using saved slides from the MEFO experiments estimates could be made of the slide offset positions that are needed for defining the non-uniformity correction at the 1 mm scale in Mason et al. (2015). Listed in Table S5 are the  $f_{nu,1mm}$  correction factors applied to the MEFO samples based on the slide offset positions. Data were not taken on the non-uniformity within the field-of-view during the freezing experiments ( $f_{nu,0.10-0.25 mm}$ ) for the MEFO collections, and hence, no correction was applied to the MEFO samples for non-uniformity at the 0.25-0.1 mm scale. On the basis of Mason et al. (2015), cf. Fig. 8 of that paper, and calculations using the factors found for CSU and Kansas sampling, the inability to quantify  $f_{nu,0.10-0.25 mm}$  will lead to an under-prediction of  $n_{INPs}(T)$  by a factor that depends on the frozen fraction of droplets at any temperature, perhaps as high as 1.7 for the first drops freezing (1 of ~50-100, or 1-2% frozen fraction) but less than 1.1 once 25% of droplets have frozen."*

220

**Reviewer's minor comment [2]:**

lines 267-268: See my above example regarding the storage issue. '(not shown)' is a very unsatisfactory parenthetical. Perhaps a better description could be made. e.g.,

225 X randomized samples were tested for storage effects by freezing before and after Y days/weeks/months of storage and showed no statistically significant.....

**Authors' response to comment [2]:**

230 Please see our response to general comment [1]. There is already a strong past basis in the literature for not expecting frozen storage to be an issue for the conditions represented in this paper, and some of the authors are preparing material on this topic for a future paper.

**Reviewer's minor comment [3]:**

235 line 464: 'holding for hours at one temperature' The wording is strange here.

**Authors' response to comment [3]:**

We agree.

**Changes in manuscript re: comment [3]:**

240 We have revised the statement to read, "*achieved when droplets remain at a single temperature for periods longer than seconds to minutes*"

**Reviewer's minor comment [4]:**

245 lines 475-490 The discussion of the factor of 3 added as a line in Figure 3 should at a minimum be introduced earlier. Preferably when the figure is introduced. Furthermore, it seems a somewhat deeper discussion of the meaning of this line is missing – that could remain in the discussion. It is clear that the DeMott 2015 et al., paper suggests that this correction factor is used for field measurements of immersion freezing of natural mineral dust for the CFDC – when comparing to a parameterized model of INP. How this relates to the results from other instruments etc. is less clear (e.g., Each of these instruments may have their own c.f. with regard to the DeMott parameterization.).  
250 My best understanding is that the 'true' aerosol concentration of (mineral dust) INP as measured by the CFDC should lie somewhere between (inclusive) the 1:1 and factor 3 lines. However, this estimate is also subject to the size limitations of the instrument and parameterization (0.5-2.4 microns). Given the other instruments also operate outside of this range a deeper discussion that ties these links seems warranted. Thus, I also suggest least-squares trendlines be added to the Figure 3 panels or their exclusion defended (For example these trends are essentially explored in Figure 4, but the link is not explicit). Fitting the Figure 3 data by eye, it appears that any trendline would be steeper than the 1:1 line. Is this truly systematic? Are there potentially different explanations for the different instruments? Including at least representative error bars in panels a-c may also assist the discussion.

**Authors' response to comment [4]:**

265 We disagree on this point. The *cf* clearly relates only to the CFDC and it is used in figures where other method results are compared to the CFDC. No one has explored if there are biases involved in measuring maximum INP number concentrations via other methods, but we do provide discussion of such possibilities in this paper. Bulk suspension immersion freezing methods are intended to capture the full aerosol size distribution and not to "miss" INPs, but other factors may come into play when a population of aerosol particles are placed into liquid. Relating different measurement methods is a multivariate problem involving limitations and potential artifact influences in all instruments, a problem for which we have tried to offer insights and a path forward for full investigation.

275 The reviewer's understanding of the DeMott et al. (2015) parameterization is not correct. The fit to determine *cf* for mineral dust particles exclusively (excluding arable soil dusts, for example) used INP activation data at higher RH to determine *cf* versus more typical RH processing values that need to be used in sampling atmospheric INPs in a regime where particles activate as water droplets prior to freezing. The value varies around  $cf = 3$ , not between  $cf = 1$  and  $cf = 3$ . This is the value that is justified for the CSU CFDC. We reference another paper on this topic and its potential source that notes 2-10 factors. Therefore, this appears a common issue with similar instruments. Until more is known, including the appropriateness of these factors for ambient INPs (likely), we wish to retain mention of the factor within the discussion section of the paper. Finally, the parameterization is applied to all sizes above 0.5

microns, not just the ones the CFDC samples. This is a common misconception, but the publication is quite clear on the use of all particles above 0.5  $\mu\text{m}$ , regardless of whether the CFDC can capture all of these or not. The reason for that was practical, for ease of application in modeling studies. Consideration for missing INPs at larger sizes was left for future study. We feel that we have otherwise provided sufficient discussion of potential size limitation effects, at least as can be warranted in this first inspection of sampling ambient INPs by different techniques. Advice is offered for future focused comparisons.

While we do not feel that a regression fit to the data in Fig. 3 adds to the demonstration of discrepancies provided in Fig. 4 and Fig. 5, we include these lines now. Are the trends systematic? Not across methods. Is that meaningful? We are not sure yet, although we have offered a number of reasons why it might be, at least for the type of sampling conducted in this paper. Are there other explanations we have not thought of? That seems a topic for future research. The regression fits in each panel of Fig. 3 now show a general trend for each method versus the CFDC, although we point out that the imposition of this fit adds no special valuable information regarding exactly what is going on. In contrast, the 1:1 line in Fig. 3 is meaningful as the basis for extrapolating perfect agreement of the CFDC with other measurements, and the 3\*CFDC line is meaningful for exploring whether the CFDC instrument underestimates all natural INPs by the factor that has been reported for mineral dust particles in the laboratory and field. Figures 4 and 5 are used to discuss the discrepancies between methods as a function of temperature, and these inspections reveal discrepancies that are not truly linear or understood from the regressions in Fig. 3. Finally, we spent a great deal of effort in the paper to explain that perfect overlap of samples was a difficult task that requires a lot coordination on the part of groups volunteering their effort in this case, with the consequence that only a small amount of data truly appropriate for statistical tests was acquired. When showing data without perfect temporal overlap, we feel that the discussion should be a bit more general. Figures 4 and 5 provide this. This paper is the start toward what would be necessary for more exact comparisons in the future.

**Changes in manuscript re: comment [4]:**

The new figures appear at the end of this response, as they will be shown in the final article. At the point of introducing these fits (first mention of trend lines in section 3.2) we write:

*“The linear relational slope between IS and CFDC data shown by the light gray dashed line in Fig. 3a. The same representation is applied in all panels of Fig. 3. We provide these fits only to show general trends between the different data sets and do not provide fit parameters herein because a deeper consideration of the source of discrepancies requires additional inspection of trends as a function of temperature, which follows below.”*

**Reviewer’s minor comment [5]:**

Figure 1. Please be explicit (throughout text) with regard to the confidence intervals. Poisson error, Gaussian?

**Authors’ response to comment [5]:**

Done.

**Changes in manuscript re: comment [5]:**

More detail describing the confidence intervals is provided now in the discussion of the individual instruments, and consolidated in Section 2.

**Reviewer’s minor comment [6]:**

Figure S1. Using  $n_{mp}$  as the y-axis label maybe confusing. The upper points are actually INP per concentrated liter of sampled air if I understand correctly.

**Authors’ response to comment [6]:**

We thought that the description in the caption might be enough to make this clear to readers, but have amended that as best possible. The axis should be consistent, in that it is always a number per unit volume, concentrated in one case and not in the other.

**Changes in manuscript re: comment [6]:**

We rephrase the caption as, “Aerosol Concentrator calibration check at  $-30^{\circ}\text{C}$  at CSU on May 19, 2016. This is a typical experimental sampling period at one temperature. In this figure, the lower data points are INP number concentrations without using the aerosol concentrator. Alternating periods of high INP number concentrations are

during use of the aerosol concentrator. Inspection of the ratio between the INP number concentrations per volume of air during periods on versus off the concentrator reveal the CF factor, which is ~90 in this case. The shaded lower region is the limit of significance for INP concentrations, as described in Section 2.1 of the manuscript.”

340

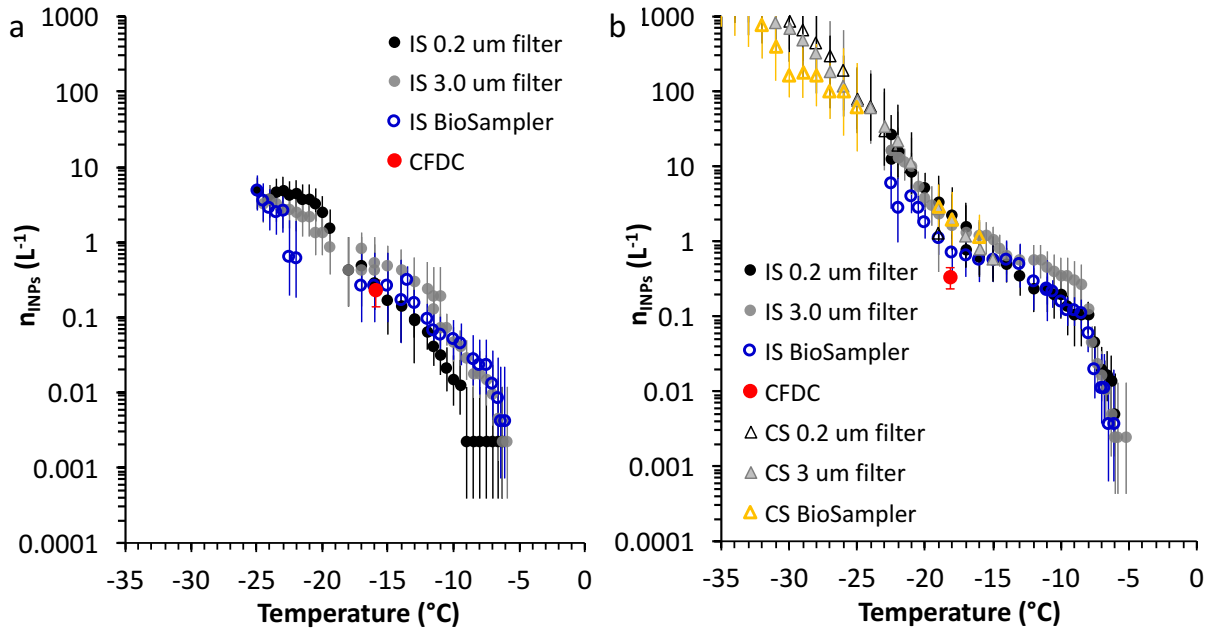


Figure 1.

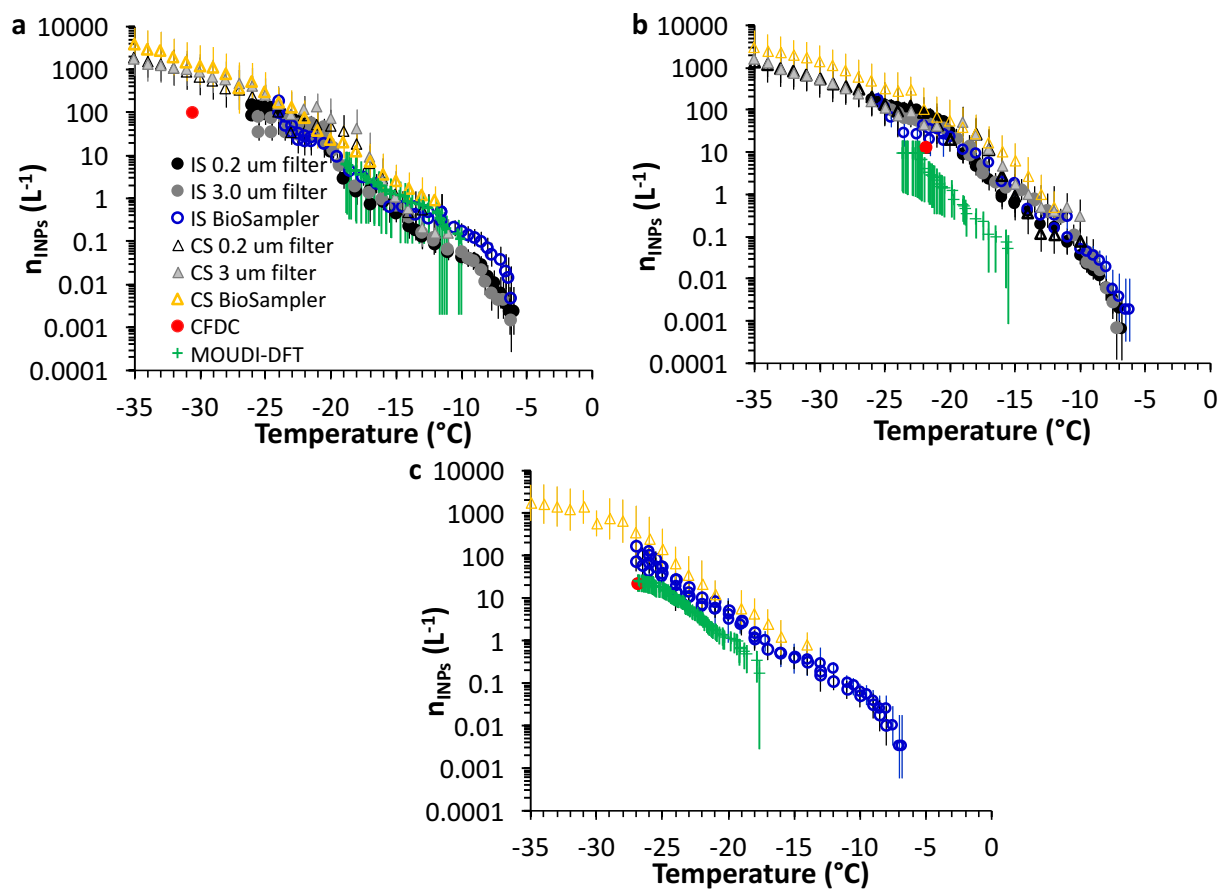
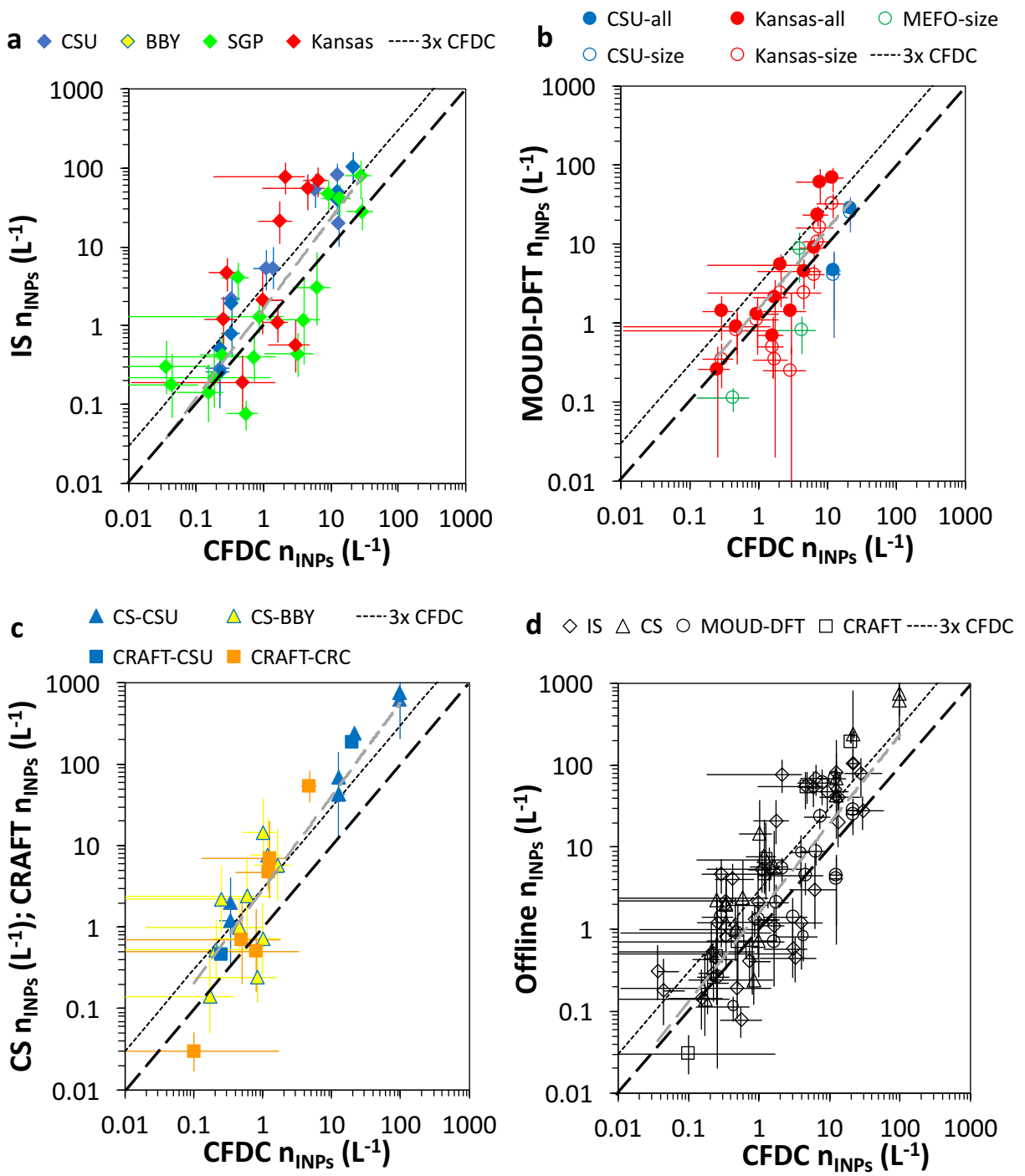


Figure 2.



345

Figure 3.

# Comparative measurements of ambient atmospheric concentrations of ice nucleating particles using multiple immersion freezing methods and a continuous flow diffusion chamber

Paul J. DeMott<sup>1</sup>, Thomas C. J. Hill<sup>1</sup>, Markus D. Petters<sup>2</sup>, Allan K. Bertram<sup>3</sup>, Yutaka Tobo<sup>4,5</sup>, Ryan H. Mason<sup>3</sup>, Kaitlyn J. Suski<sup>1,6</sup>, Christina S. McCluskey<sup>1</sup>, Ezra J. T. Levin<sup>1</sup>, Gregory P. Schill<sup>1</sup>, Yvonne Boose<sup>7</sup>, Anne Marie Rauker<sup>1</sup>, Anna J. Miller<sup>8</sup>, Jake Zaragoza<sup>1,9</sup>, Katherine Rocci<sup>10</sup>, Nicholas E. Rothfuss<sup>2</sup>, Hans P. Taylor<sup>2</sup>, John D. Hader<sup>2</sup>, Cedric Chou<sup>3</sup>, J. Alex Huffman<sup>11</sup>, Ulrich Pöschl<sup>12</sup>, Anthony J. Prenni<sup>13</sup>, and Sonia M. Kreidenweis<sup>1</sup>

<sup>1</sup>Department of Atmospheric Science, Colorado State University, Fort Collins, CO, 80523, USA

<sup>2</sup>Department of Marine, Earth and Atmospheric Sciences, North Carolina State University, Raleigh, NC, 27695 USA

<sup>3</sup>Department of Chemistry, University of British Columbia, Vancouver, BC, V6T1Z1, Canada

<sup>4</sup>National Institute of Polar Research, 10-3 Midori-cho, Tachikawa, Tokyo, 190-8518, Japan

<sup>5</sup>Department of Polar Science, School of Multidisciplinary Sciences, SOKENDAI (The Graduate School for Advanced Studies), Tachikawa, 190-8518 Tokyo, Japan

<sup>6</sup>Now at Pacific Northwest National Laboratory, Richland, WA, 99352, USA

<sup>7</sup>Karlsruhe Institute of Technology, Institute of Meteorology and Climate Research (IMK-IFU), 82467 Garmisch-Partenkirchen, Germany

<sup>8</sup>Department of Chemistry, Reed College, Portland, OR, 97202, USA

<sup>9</sup>Now at Air Resource Specialists, Fort Collins, CO, 80525, USA

<sup>10</sup>Department of Earth Sciences, University of New Hampshire, Durham, NH, 03824, USA

<sup>11</sup>Department of Chemistry & Biochemistry, University of Denver, Denver, CO, 80210, USA

<sup>12</sup>Department of Multiphase Chemistry, Max Planck Institute for Chemistry, D-55128, Mainz, Germany

<sup>13</sup>National Park Service, Air Resources Division, Lakewood, CO, 80228, USA

*Correspondence to:* Paul J. DeMott (Paul.Demott@Colostate.edu)

**Abstract.** A number of new measurement methods for ice nucleating particles (INPs) have been introduced in recent years, and it is important to address how these methods compare. Laboratory comparisons of instruments sampling major INP types are common, but few comparisons have occurred for ambient aerosol measurements exploring the utility, consistency and complementarity of different methods to cover the large dynamic range of INP concentrations that exists in the atmosphere. In this study, we assess the comparability of four offline immersion freezing measurement methods (Colorado State University Ice Spectrometer, IS; North Carolina State University Cold Stage, CS; National Institute for Polar Research Cryogenic Refrigerator Applied to Freezing Test, CRAFT; University of British Columbia Micro-Orifice Uniform Deposit Impactor – Droplet Freezing Technique, MOUDI-DFT) and an online method (continuous flow diffusion chamber, CFDC) used in a manner deemed to promote/maximize immersion freezing, for the detection of INP in ambient aerosols at different locations and in different sampling scenarios. We also investigated the comparability of different aerosol collection methods used with offline immersion freezing instruments. Excellent agreement between all methods could be obtained for several cases of co-sampling with perfect temporal overlap. Even for sampling periods that were not fully equivalent, the deviations between atmospheric INP number concentrations measured with different methods were mostly less than one order of magnitude. In some cases, however, the deviations were larger and not explicable without sampling and

390 measurement artifacts. Overall, the immersion freezing methods seem to effectively capture INP that activate as single particles in the modestly supercooled temperature regime ( $>-20^{\circ}\text{C}$ ), although more comparisons are needed in this temperature regime that is difficult to [access](#) with online methods. Relative to the CFDC method, three immersion freezing methods that disperse particles into a bulk liquid (IS, CS, CRAFT) exhibit a positive bias in measured INP number concentrations below  $-20^{\circ}\text{C}$ , increasing with decreasing temperature. This bias was present, 395 but much less pronounced for a method that condenses separate water droplets onto limited numbers of particles prior to cooling and freezing (MOUDI-DFT). Potential reasons for the observed differences are discussed, and further investigations [proposed](#) to elucidate the role of all factors involved.

## 1 Introduction

Heterogeneous ice nucleation by atmospheric aerosols impacts the microphysical composition, radiative properties and precipitation processes in clouds colder than  $0^{\circ}\text{C}$ . These interactions are complex, and any first assessment of 400 the role of different particles on ice formation, cloud properties and climate requires more observations of ice nucleating particles (INPs, as defined by Vali et al., 2015) present in ambient air. To quantify the initial stage of ice nucleation in the atmosphere, multiple sampling techniques are now being used in field studies (Hader et al., 2014; Mason et al., 2015; DeMott et al., 2015; Stopelli et al., 2015; Boose et al., 2016; Schrod et al., 2016a,b). Since these 405 various measurements are being used as bases for developing numerical model parameterizations for different emission sources, their comparability should be assessed. In this study, we focus on ice nucleation measurements in the mixed-phase cloud temperature regime ( $0$  to  $-38^{\circ}\text{C}$ ), where heterogeneous ice nucleation is the only trigger for primary ice initiation. Within this regime, INP number concentration can increase up to 10 orders of magnitude as temperatures cool from  $-5$  to  $-35^{\circ}\text{C}$  (DeMott et al., 2015; DeMott et al., 2016; Hiranuma et al., 2015; Murray et al., 410 2012; Petters and Wright, 2015), and there can be up to 2-3 orders of magnitude of temporal and spatial variability at a single temperature by any given method (DeMott et al. 2010; Petters and Wright, 2015).

This study compares results from an online INP measurement method used over the last 25 years, the Colorado State University (CSU) continuous flow diffusion chamber (CFDC), with four offline immersion freezing methods for INP measurements. These four variants immerse particles into variously-sized liquid volumes/droplets which are 415 cooled to freezing in different ways in order to measure the immersion freezing INP number per volume of air. In this study, comparisons are made only for times when the CFDC instrument operated in a manner which emphasized immersion freezing contributions to ice nucleation (DeMott et al., 2015). A principal reason to evaluate consistency between approaches, and in ambient air, is because offline methods collect large enough sample volumes to estimate INP number concentrations active at modest supercooling (as warm as  $-5^{\circ}\text{C}$ ), [a temperature regime](#) where online 420 instruments are unable to obtain statistically significant data samples. [In contrast, online methods can provide high time resolution data at lower temperatures.](#) Comparability between off- and online methods can be assessed in temperature regions of overlap. Another reason for such a comparison is to gauge the magnitude of uncertainties when only a single INP measurement method is used or when data sets from different instruments are combined toward addressing a scientific question. This study differs from previous efforts in that comparisons have been

425 restricted to the ambient atmosphere, where presumably the compositions of INPs are more diverse and likely  
different than for single INP types often examined in laboratory studies. In one set of laboratory studies (Hiranuma  
et al., 2015), discrepancies between online and offline methods were noted for sampling NX-illite INPs. In  
particular, bulk, offline freezing methods estimated INP ice nucleation efficiencies that were 10 to 1000 times lower  
than found with continuous flow chambers and the AIDA (Aerosol Interaction and Dynamics in the Atmosphere)  
430 expansion cloud chamber for temperatures warmer than about  $-25^{\circ}\text{C}$ . Similar discrepancies were discussed by  
Emersic et al. (2016). Impacts of dry dispersion versus wet immersion on the agglomeration properties and the  
exposures of active sites were implicated in varied ways in both studies for explaining discrepancies. Grawe et al.  
(2016) also noted discrepancies occurring in single particle activation via immersion freezing in the LACIS (Leipzig  
Aerosol Cloud Interaction Simulator) instrument for certain, but not all, combustion ash particles. In contrast, no  
435 discrepancies were reported in processing wet dispersed ice nucleating bacteria from Snomax® (Wex et al., 2014).  
Nevertheless, many of the reported laboratory results have thus far focused on a specific INP type that was shared  
across laboratories and for which individual investigators were allowed to determine protocols for generation as an  
aerosol or production of liquid suspensions for the different methods used. Here, by contrast, we focus on co-located  
sampling of ambient aerosol, for which no more than two methods have hitherto been used in a single published  
440 study using this approach.

The goal of this inter-comparison is to assess the status and potential for using single or combinations of INP  
measurement methods to access and measure the dynamic range of atmospheric INP concentrations active for ice  
initiation in mixed-phase clouds. The assessment assumes that the time-dependence is subordinate to the  
temperature dependence of the freezing nucleation process. The scientific basis of this assumption and its  
445 implications for the assessment are discussed. We address the magnitude of agreement, how particle collection  
methods may influence immersion freezing measurements, and whether obvious biases appear, for example due to  
the different size ranges of particles that may be collected in offline and online measurement systems. This study is  
not intended as a comprehensive evaluation, but rather a first assessment using some of the most common methods  
likely to be applied for atmospheric sampling in the coming years.

## 450 **2 Methods**

Several INP measurement methods, most with a legacy of previous atmospheric measurements, are herein inter-  
compared during sampling of ambient aerosols. This section describes the instruments, details of sampling protocol  
and processing, and sampling sites.

### **2.1 INP measurement systems**

#### 455 **2.1.1 Colorado State University CFDCs**

Online INP measurements were made with two CSU CFDCs, designed for mobile and aircraft deployments, but  
otherwise identical (Eidhammer et al., 2010; DeMott et al., 2015). As described in these previous publications,  
aerosol flows vertically downward in a central lamina between concentric, cylindrical walls that are ice coated and

thermally controlled at different temperatures. Setting a temperature difference between the colder (inner) and warmer (outer) ice walls in the upper “growth” region establishes a nearly steady-state relative humidity where ice nucleation and ice crystal growth can occur over a few seconds. The temperatures of the inner and outer walls are set to the same value in the lower “evaporation” region of the chamber, which promotes evaporation of water droplets and wet aerosols, but retains activated ice particles at larger sizes that can be detected as optically-distinct for counting as INPs with an optical particle counter. For this study, the aerosol lamina was 15% of the total volumetric flow of 10 L min<sup>-1</sup>. Filtered and dried air was recirculated as sheath flow (8.5 L min<sup>-1</sup>). Also for this study, a nominal water-supersaturated condition of 105% RH was chosen for operation at all temperatures. This selection was made to force activation of cloud droplets on aerosols at temperatures where some proportion could freeze during the transit time in the instruments, allowing for the most direct comparison possible to the offline immersion freezing methods. Previous studies have explored the need to set the RH in CFDC style instruments to values far above that expected in natural clouds (100-101% RH) in order to mimic this freezing process (Petters et al., 2009; DeMott et al., 2010; 2015). Although DeMott et al. (2015) showed in laboratory studies that operational RH up to 109% might be required for full expression of freezing in the CFDC, 105% is the value that has been consistently used in field studies so that liquid droplets do not survive through the evaporation region and be counted as false positive INPs. For mineral dusts, at least, operation at 105% could miss up to a factor of 3 (DeMott et al., 2015) INP number concentrations that ultimately activate via immersion freezing or some combination of nucleation mechanisms. It is unknown if this factor exists for all INP types. Hence, no correction factor was applied to the CFDC data here, but the implications of the factor of 3 will be discussed. [CFDC measurement uncertainties vary with processing conditions, and are typically ±0.5°C and 2.4% water relative humidity at -30°C \(DeMott et al., 2015\).](#)

Aerosol particles at sizes that might confound optical detection of (i.e., be mistakenly counted as) ice crystals were removed upstream of the CFDC using dual single-jet impactors set to a cut-point aerodynamic diameter of 2.4 μm. This creates a sampling bias for the CFDC versus other systems that capture larger particles for immersion freezing experiments, but is required to assure detection of activated ice crystals that typically exit the CFDC at optical diameters approximately >4 μm.

Interval periods of sampling filtered air within the overall sampling period were used to correct for any background frost influences on INP counts. [We follow Schill et al. \(2016\) for correcting sample concentrations for background and for defining confidence intervals for CFDC data, which are represented by error bars in presented plots. Specifically, corrected INP concentrations are the sample concentrations with the interpolated background concentrations subtracted. The standard deviation derived from the Poisson counting error during both the sample and the interpolated background concentrations were added in quadrature to obtain the INP concentration error.](#) Concentrations are considered significant if they are 1.64 times larger than the INP concentration error, which corresponds to the Z statistic at 95% confidence for a one-tailed distribution. Consequently, although the lowest limit of detection for 10-min sampling intervals is ~0.2 L<sup>-1</sup>, significant data often requires in excess of 1 L<sup>-1</sup> INP concentrations. As a special sampling aide in these studies, an aerosol concentrator (Model 4240, MSP Corporation) was used upstream of the CFDC in some cases to enhance INP number concentrations and facilitate statistically significant quantification of INP number concentrations. The enhancement of aerosol concentrations using this dual

virtual impactor method affects only particles of diameter  $>0.5 \mu\text{m}$  and varies from a factor of 10 at this diameter up to a factor of about 140 at sizes above  $1 \mu\text{m}$  (Tobo et al., 2013). The concentration factor achieved for ambient INPs then depends on the INP size distribution, which is difficult to know a priori. The methods outlined in Tobo et al. (2013) were followed to define the concentration factor, using the ratio of CFDC INP number concentrations with and without the concentrator under conditions where statistical significance of measurement was achieved without the concentrator. This was assessed over the term of measurements for each site in the study, and applied to all CFDC data when using the aerosol concentrator. An example of measurements on and off of the concentrator for one of the sampling periods used in this study is shown in the Supplement, Fig. S1. Use of the aerosol concentrator is indicated in individual cases in the data tables, also included in the Supplement.

500

Particle losses in upstream tubing, the aerosol impactor, and the inlet manifold of the CFDC have previously been estimated as 10% for particles with diameter  $0.1$  to  $0.8 \mu\text{m}$  (Prenni et al., 2009), and we apply this correction to data for this paper.

505

### 2.1.2 North Carolina State University CS

The design of the North Carolina State University (NC State) cold stage-supported droplet freezing assay (CS) and data reduction methods are described in detail in Wright and Petters (2013) and Hader et al. (2014).

Droplet populations of three distinct droplet size ranges may be investigated in the CS; these are termed pico-, nano-, and microdrops. Pico-drops are generated by mixing a  $15 \mu\text{L}$  aliquot of bulk suspension (particles placed into liquid by methods outlined below) with squalene and emulsifying the hydrocarbon-water mixture using a vortex mixer. The emulsion is poured into the CS sample tray, consisting of an aluminum dish holding a hydrophobic glass slide. Approximately 400 to 800 droplets with a typical diameter of  $\sim 85 \mu\text{m}$  are analyzed in this manner for each collected sample. Nanodrops are generated by manually placing drops with a syringe needle tip on a squalene covered glass slide and letting the drops settle to the squalene-glass interface. Approximately 80 droplets are typically analyzed per experiment with a typical diameter of  $\sim 660 \mu\text{m}$ . Microdrops are placed directly on the hydrophobic glass slide using an electronic micropipette. In contrast to the pico- and nanodrops, these drops are in contact with gas-phase composed of dry  $\text{N}_2$ . Up to 256 drops of diameter  $\sim 1240 \mu\text{m}$  ( $1 \mu\text{l}$ ) can be investigated in a single experiment. For all experiments, the CS was cooled at a constant rate of  $1^\circ\text{C min}^{-1}$  ( $2^\circ\text{C min}^{-1}$  at Bodega Marine Laboratory) and the number of unfrozen drops was recorded using a microscope in increments of  $dT = 0.17^\circ\text{C}$  resolution. Temperature uncertainty is based on the manufacturer's (Model TR141-170, Oven Industries) stated tolerance of the cold plate thermistor ( $\pm 1^\circ\text{C}$ ). To account for slightly higher temperatures of the squalene relative to the glass slide, a temperature calibration was applied to the drop freezing data (Hader et al., 2014). The resulting data were inverted to find the cumulative concentration of INPs ( $C_{INPs}(T)$ ) per volume of liquid at temperature,  $T$ , using the method of Vali (1971),

515

520

525

$$C_{INPs}(T) = -\left(\frac{1}{V}\right) \ln\left(\frac{N_u(T)}{N}\right) \quad (1)$$

where  $N_u$  is the unfrozen number of an initial  $N$  liquid entities (droplets in this case) of volume  $V$ . Conversion to number concentration of INPs per volume of air ( $n_{INPs}(T)$ ) is determined by,

530

$$n_{INPs}(T) = C_{INPs}(T) \left( \frac{V_w}{V_s} \right) \quad (2)$$

where  $V_w$  is the volume of liquid suspension (same units as used to compute  $C_{INPs}(T)$ ) and  $V_s$  is the sample volume (L) of air collected.

535 To minimize sample heterogeneity, only droplets with  $78 \mu\text{m} < D_p < 102 \mu\text{m}$  were included in the calculation of  $n_{INPs}(T)$  for picodrops. No restriction was applied to the nanodrops or microdrops. Furthermore, the warmest two percent of data were removed after the calculation of  $C_{INPs}(T)$  but before plotting for the pico- and nanodrops due to large uncertainty stemming from poor counting statistics (Hader et al., 2014). The INP content of the ultrapure water (see section 2.2) was measured in the above manner between  $-20^\circ\text{C}$  and  $-35^\circ\text{C}$ . The effective INP content was  
 540 determined by subtracting the background INP numbers from the ultrapure water from observed  $n_{INPs}(T)$ . No impurities were detected at  $T > -20^\circ\text{C}$ . Analysis of CS repeat trial data involved binning data into  $1^\circ\text{C}$  intervals. Confidence intervals were calculated using two standard deviations of the geometric mean for each bin where multiple data points were available.

### 2.1.3 University of British Columbia MOUDI-DFT

545 The second immersion freezing method involved freezing of droplets grown on substrate-collected particles in a temperature and humidity controlled flow cell (Mason et al., 2015) and is referred to as the droplet freezing technique (DFT). A micro-orifice uniform deposit impactor (MOUDI; MSP Corp.) was used to size-select particles from known volumes of air onto a substrate for direct DFT analysis in a number of cases (MOUDI-DFT, Mason et al., 2015). The MOUDI collected size-selected particles onto multiple hydrophobic glass cover slips (HR3-215; Hampton Research). For the measurements performed in Kansas, United States, stages 2-9 of the MOUDI were  
 550 used corresponding to particle size bins of 10–5.6, 5.6–3.2, 3.2–1.8, 1.8–1.0, 1.0–0.56, 0.56–0.32, 0.32–0.18, and 0.18–0.10  $\mu\text{m}$  (50% cutoff aerodynamic diameter; Marple et al., 1991), respectively. For the measurements at CSU, stages 2-8 were used and for the measurements at Manitou (Colorado) Experimental Forest Observatory (MEFO), stages 2–7 were used.

555 For DFT analysis, droplets were grown in the flow cell by decreasing temperature to  $0^\circ\text{C}$  and passing a humidified flow of He gas over the slides. Water was allowed to condense until approximately  $100 \mu\text{m}$  diameter water droplets formed on the collected particles, typically covering several to some tens of particles depending on loading. Droplets were then monitored for freezing using a coupled optical microscope (Axiolab; Zeiss, Oberkochen, Germany) with a  $5\times$  magnification objective, as temperature was lowered at a constant rate. A CCD camera connected to the optical  
 560 microscope recorded a digital video while a resistance temperature detector recorded the temperature. A cooling rate of  $10^\circ\text{C min}^{-1}$  (from  $0^\circ\text{C}$  to  $-40^\circ\text{C}$ ) was used in these studies to either minimize freezing of droplets due to contact of a growing crystal or minimize evaporation of unfrozen droplets due to the Bergeron-Findeisen process, i.e. growth of the existing ice crystals at the expense of the surrounding liquid droplets (Mason et al., 2015). The liquid droplet may evaporate or the frozen droplet will grow towards and eventually contact a liquid droplet, causing it to freeze. If  
 565 a droplet is lost to evaporation or to non-immersion freezing, two assumptions are made:

1) That the droplet contained an INP and would have frozen by immersion (on its own) at the same temperature as the non-immersion/evaporation event. This gives an upper limit to the calculated INP concentration

2) That the droplet contained no INPs and would not have frozen until homogeneous temperatures, which are around -36°C in the flow cell used. This assumption provides a lower limit to the calculated INP concentration at a given T.

570 The method to obtain the INP number concentrations in air follows a similar basis as for the CS, but with modest differences as,

$$n_{INPs}(T) = -\ln\left(\frac{N_u(T)}{N}\right) N \left(\frac{A_{deposit}}{ADFTV_s}\right) f_{nu} f_{ne} \quad (3)$$

where  $N$  is the total number of droplets condensed onto the sample in this case,  $A_{deposit}$  is the total area of the sample deposit on the hydrophobic glass cover slip,  $ADFT$  is the area of the sample monitored in the digital video during the droplet freezing experiment,  $V$  is the volume of air sampled by the MOUDI.  $f_{ne}$  is a correction factor to account for the statistical uncertainty that results when only a limited number of nucleation events are observed.  $f_{ne}$  was calculated following the approach given in Koop et al., (1997) using a 95% confidence interval.  $f_{nu}$  is a correction factor to account for non-uniformity in particle concentration across each MOUDI sample (Mason et al., 2015; Mason et al., 2016). This later correction factor consists of two multiplicative terms:  $f_{nu,1mm}$  and  $f_{nu,0.25-0.10 mm}$ , with these terms correcting for non-uniformity in the particle deposits at the 1 mm and 0.25-0.1 mm scale, respectively. Since only a small area (1.2 mm<sup>2</sup>) of the particle deposits are analyzed and the concentration of particles are not uniform across the entire substrate,  $f_{nu,1mm}$  needs to be applied. Since the concentration of particles are not uniform within the small area of the particle deposits analyzed for freezing,  $f_{nu,0.25-0.10 mm}$  needs to be applied. Listed in Tables S3 and S4 are the  $f_{nu,1mm}$  and  $f_{nu,0.25-0.10mm}$  values applied to the MOUDI-DFT samples collected at CSU and Kansas, respectively. Different correction factors were used for the CSU and Kansas samples since different substrate holders were used to position the glass slides within the MOUDI at the two sites. Substrate holders were not yet employed during the earlier MEFO studies (Huffman et al., 2013). However, using saved slides from the MEFO experiments estimates could be made of the slide offset positions that are needed for defining the non-uniformity correction at the 1 mm scale in Mason et al. (2015). Listed in Table S5 are the  $f_{nu,1mm}$  correction factors applied to the MEFO samples based on the slide offset positions. Data were not taken on the non-uniformity within the field-of-view during the freezing experiments ( $f_{nu,0.10-0.25 mm}$ ) for the MEFO collections, and hence, no correction was applied to the MEFO samples for non-uniformity at the 0.25-0.1 mm scale. On the basis of Mason et al. (2015), cf. Fig. 8 of that paper, and calculations using the factors found for CSU and Kansas sampling, the inability to quantify  $f_{nu,0.10-0.25 mm}$  will lead to an under-prediction of  $n_{INPs}(T)$  by a factor that depends on the frozen fraction of droplets at any temperature, perhaps as high as 1.7 for the first drops freezing (1 of ~50-100, or 1-2% frozen fraction) but less than 1.1 once 25% of droplets have frozen.

Confidence intervals (95%) were calculated based on the Poisson distribution, following Koop et al. (1997). These intervals are nearly equivalent to Binomial confidence intervals for the data in this study.

#### 2.1.4 Colorado State University IS

600 The CSU ice spectrometer (IS) (Hill et al., 2014; Hill et al., 2016; Hiranuma et al., 2015) measures freezing in an array of liquid aliquots held in a temperature-controlled block. For IS processing, aerosol particles in suspensions are distributed into 24 to 48 aliquots of 40-80 μL held in sterile 96-well PCR trays (μCycler, Life Science Products). The numbers of wells frozen are counted at 0.5 or 1°C intervals during cooling at a rate of 0.33°C min<sup>-1</sup>.

605 Temperature was measured with 0.1°C resolution and 0.4°C accuracy (Hill et al., 2016). Calculation of  $n_{INPs}(T)$  was made using Eqs. (1) and (2), where  $V$  was the aliquot volume. Control wells of ultrapure water (see section 2.2) were also cooled, and correction for any frozen aliquots in the pure water control versus temperature was made in all cases, similar to the CS method. Binomial sampling confidence intervals (95%) were determined for IS data, as described in Hill et al. (2016).

### 2.1.5 National Institute of Polar Research CRAFT

610 The Cryogenic Refrigerator Applied to Freezing Test (CRAFT) device has been described in detail by Tobo (2016). CRAFT is a classical cold plate device akin to the DFT and the CS instruments, but involves procedures to assure sample isolation, primarily from the cold plate surface using a layer of Vaseline®. Droplets containing collected aerosols are pipetted in a clean hood onto the coated aluminum plate that is then set on the stage of a portable Stirling-engine-based refrigeration device (CRYO PORTER, Model CS-80CP, Scinics Corporation). The freezing device is also operated in a booth that is aspirated with clean air. The temperature of the plate was measured using a  
615 single temperature sensor, and the uncertainty of temperature is 0.2°C.

For each CRAFT measurement, 49 droplets with a volume of 5 µL were used and the temperature was lowered at a rate of 1°C min<sup>-1</sup> until all the droplets froze. Results of control experiments with pure water droplets were used to correct for any contamination introduced by water. Each freezing experiment was monitored by a conventional  
620 video camera. Video image analysis was used to establish the number fractions of droplets frozen and unfrozen at 0.5°C intervals. Analyses of  $n_{INPs}(T)$  followed the same scheme as used for the CS and IS measurements. Binomial confidence intervals (95%) were determined, as for the IS data.

## 2.2 Aerosol collection methods and processing for immersion freezing studies

At different times, ambient aerosol samples were collected directly into liquid or onto filters, for subsequent  
625 resuspension into liquid. Collection directly into liquid was done using a glass Bioaerosol sampler (SKC Inc.), hereafter termed the BioSampler. This unit was typically placed on a table at 1.2 m above ground level. The BioSampler directs particles into a sample cup filled with 20 mL of ultrapure water (18.2 MΩ cm resistivity and 0.02 µm filtered using an Anotop syringe filter (Whatman, GE Healthcare Life Sciences)) where they impinge to form an aqueous suspension. Particle collection efficiencies for this technique exceed 80% for particles larger than  
630 200 nm and approach 100% for particles larger than 1 µm (Willeke et al., 1998). Particles with diameter  $D_p > 10$  µm are expected to impact the inlet wall (Hader et al., 2014). Sample flow rate was 12.5 L min<sup>-1</sup>, and impaction liquid was replenished every 20-30 min by adding ultrapure water into the collection cup.

For IS-only and some shared samples, particles were also collected onto pre-sterilized 47 mm diameter Nuclepore™ track-etched polycarbonate membranes (Whatman, GE Healthcare Life Sciences). Filters were pre-  
635 cleaned by soaking in 10% H<sub>2</sub>O<sub>2</sub> for 10 min, followed by three rinses in ultrapure water, and were dried on foil in a particle-free, laminar flow cabinet. Filters were held open-faced in sterile Nalgene filter units (Thermo Scientific, Rochester, NY). Flow rates varied from about 8 to 13 L min<sup>-1</sup> for ambient temperature and pressure conditions in different studies. Collection onto 0.2 µm pore-diameter filters was typical, although comparison versus 3 µm pore-

diameter filters was also done in some initial experiments. Both filter types were of ~10  $\mu\text{m}$  average thickness and 15% porosity. On the basis of theoretical collection efficiencies (Spurny and Lodge, 1972), the 0.2  $\mu\text{m}$  pore filters should have collected particles of all sizes with very high efficiency, the lowest efficiency being at about 0.1  $\mu\text{m}$  (~80%). In contrast, the filters with 3  $\mu\text{m}$  pores are expected to collect 15% and 55% of all particles at sizes of 0.4 and 1  $\mu\text{m}$ , respectively, increasing to >75% collection at sizes above 1.5  $\mu\text{m}$ . In this manner, the larger pore size emphasizes the contributions of supermicron aerosols to immersion freezing INPs.

After particle collection, filters were stored frozen at -25 or -80°C in sealed, sterile petri dishes until they could be processed (few hours to few months). Biosampler samples were similarly stored frozen and processed over similar time frames. MOUDI collections for the DFT method were vacuum-sealed after collection, stored at 4°C in a refrigerator, shipping was done with cold packs prior to cold-stage flow cell measurements at the University of British Columbia. We therefore assume similar impacts, if any, of storage on INPs following thawing for processing.

This study was not initially conceived as one to test storage impacts on INPs, which should be addressed in future research. We do not expect storage methods to impact result on the basis of existing documentation in the literature. For example, in their study of INPs in rainwater, Petters and Wright (2015) noted that the argument that INP activity remains unaltered by the freezing of samples and subsequent storage for some time is at the core of the general application of immersion freezing methods. They noted, with reference to other literature, the generally better than 1°C repeatability of freezing temperatures for droplets that undergo repeated freeze/thaw cycles.

For processing of INP freezing spectra, filters were transferred to sterile, 50 mL Falcon polypropylene tubes (Corning Life Sciences), immersed in 7.0-10.0 mL of ultrapure water, and tumbled for 30 min in a rotator (Roto-Torque, Cole-Palmer) to suspend particles in liquid. Common liquid suspensions were shared amongst methods in some cases (see section 2.3), following freezing and shipping to different investigators. We detected no measurable impact of processing rinsed suspensions immediately versus after freezing of the bulk water, mostly supported by other recent studies (Beall et al., 2017). We will note that while all immersion freezing methods performed tests comparing freezing of the liquid samples and the purified water used in their setups, and corrected for pure water freezing events, no correction is made for any INPs that might be released from the filters used for collection. We have found that filters release a modest number of INPs active at lower temperatures, even after the pre-cleaning with H<sub>2</sub>O<sub>2</sub> and purified water. A detailed analysis of this will be presented in a future publication. The percentages of undiluted INPs due to such contamination is ~3 % in the -25 to -30°C range, and since immersion freezing measurements at these temperatures require dilution of liquid samples by 100 to 3000 times, we neglected any corrections.

### 2.3 Sampling sites/periods and objectives

Sampling sites represent a variety of ecosystems, climates and elevations across the Western U.S., including agricultural regions of the U.S. High Plains, intermountain desert regions, and a coastal site. The majority of data included in this inter-comparison involved periods that did not include all groups and were not temporally-aligned for all instrument systems. Nevertheless, substantial overlap of sampling periods occurred in all cases. Very often,

675 the CFDC sampling was conducted to obtain data at multiple temperatures, while offline collections were made for longer periods to obtain integrated INP temperature spectra. Times when the sampling periods were the same for the offline systems and for the CFDC, while it was operating at a single temperature, are listed in Table 1. Other site locations, characteristics, and instruments participating when there were overlapping sample periods are listed in Table 2.

### 680 **2.3.1 Colorado State University, Fort Collins, CO, USA**

685 Sampling was conducted outside of the Atmospheric Chemistry building at Colorado State University at different times and including different methods. The laboratory site is on a small hill on the western edge of the Fort Collins urban area, residing amongst surrounding grasslands. Initially, a series of measurement days were conducted in which collections for three immersion freezing methods were made while the CFDC sampled at a single temperature for the entire sampling period. While this protocol permitted only a single comparison point versus the temperature spectra obtained by offline measurements, the purpose was to obtain a statistically significant CFDC  $n_{INPs}(T)$  value during the course of time-integrated offline samples and to assure that any signal variance occurring during sampling was the same for all measurements. Such aligned sampling was conducted on five different days (see Table 1). Participating in these temporally-aligned experiments were the IS, CS, and MOUDI-DFT instruments. For 690 these periods, the filter sampling units, BioSampler and (when used) MOUDI sampling units were set in close proximity and at the same sampling elevation. Filter suspensions from the two pore-size (0.2 and 3.0  $\mu\text{m}$ ) filter collections and from the BioSampler were shared for IS and CS measurements. All CS data were analyzed using the pico- and nanodrop technique.

695 Sampling was also conducted at CSU without exact temporal overlap of CFDC, IS, and CRAFT method measurements, as noted in Table 2. CRAFT filters (0.2  $\mu\text{m}$  pore size) were drawn for 6 hours at a flow rate of 10 L  $\text{min}^{-1}$  at standard temperature and pressure (STP) conditions ( $T = 273 \text{ K}$ , 1013.5 mb). IS filter (0.2  $\mu\text{m}$  pore size) were drawn for 4 hours at a flow rate of 13 L  $\text{min}^{-1}$  at ambient temperature and pressure. The CFDC sample was temporally aligned with the IS sample, and single operating temperatures were used.

### **2.3.2 Northern Colorado, USA, agricultural region**

700 Sampling over previously harvested fields during Fall 2010 was conducted at a rural site approximately 26 km NNE of the CSU Atmospheric Chemistry building, at Grant Family Farms, near the village of Waverly, CO. The sampling field sites on different days, sampling protocol and the results used in the present study, are discussed in detail by Garcia et al. (2012). Sampling by CFDC and IS (BioSampler) were temporally overlapped in this study. This site is referred to as NoCO in the data tables in the Supplement.

### 705 **2.3.3 Manitou Experimental Forest, CO, USA**

Sampling within an open forest site at MEFO as part of the Bio-hydro-atmosphere interactions of Energy, Aerosols, Carbon,  $\text{H}_2\text{O}$ , Organics & Nitrogen project (Ortega et al., 2014) during Summer 2011 was conducted as described

by Huffman et al. (2013), Prenni et al. (2013) and Tobo et al. (2013). Only two selected periods from that study for which there was partial overlap of samples from the CFDC and MOUDI-DFT methods were available for this study.

#### 710 **2.3.4 Kansas, USA, agricultural region**

Sampling periods were conducted in and around the times of different crop harvesting at Kansas State University Northwest Research Extension Center in Colby, KS as part of a larger study (Suski et al., 2017). Sampling periods used for this study were during mornings before or evenings following harvesting of various crops, and during daytime near fields being harvested of soy and sorghum crops. CFDC sampling was conducted from the CSU  
715 Mobile Laboratory facility, using gasoline powered generators, as described previously by McCluskey et al. (2014). The mobile laboratory was in all cases well upwind of the generators. Aerosols were sampled through an inlet comprised of a stainless-steel rain hat with a ½" OD stainless steel tube attached. MOUDI-DFT (Mason et al., 2016) and filter samples were collected with their inlets at the same approximate elevation as the CFDC inlet, and used separate pumps for drawing samples. The CFDC scanned different temperatures during the IS filter (0.2 µm) and  
720 MOUDI-DFT sampling periods.

#### **2.3.5 Southern Great Plains (SGP), USA, site**

The site at Lamont, OK (Table 2) is the central instrumentation suite location for the U. S. Department of Energy's Atmospheric Radiation Measurement program, Southern Great Plains (SGP) field site. CFDC and IS instruments both drew air from a platform at 10 m above ground elevation at this site. Sampling occurred in a transition from dry  
725 to wet conditions in the Spring of 2014. The CFDC was operated to scan temperatures during the IS filter (0.2 µm) sampling period. A selection of representative days of data were chosen, and full study data will be included in a separate publication.

#### **2.3.6 Bodega Marine Laboratory, CA, USA**

Sampling near Bodega Bay, CA (BBY in subsequent figures) occurred during the CalWater-2015 study (Ralph et al., 2015; Martin et al., 2016). The sampling site was at the University of California, Davis Bodega Marine  
730 Laboratory, ~100 m ENE of the seashore and ~30 m north of the northernmost permanent building at the site (Martin et al., 2016). The CFDC and IS instruments sampled from approximately 4 m above the surface. The CFDC was operated to scan temperatures during the IS filter (0.2 µm) sampling period. CS BioSampler samples, overlapping with IS and CFDC sampling, were drawn from an elevation of 1 m above the vegetated surface,  
735 approximately 20 m west of the other samplers. All BBY CS data are analyzed using the microdrop technique. A few representative days are chosen from the data set for comparison of IS and CS data with CFDC data. Comparison of the complete CS and IS data sets will be included in a publication in preparation.

#### **2.3.7 Canyonlands Research Center, UT, USA**

The Nature Conservancy's Canyonlands Research Center is an intermountain (Rocky Mountains, U.S.), high desert  
740 site located adjacent to Canyonlands National Park in SE Utah. Sampling occurred in May of 2016. IS and CRAFT

filters were drawn at 1.2 m above ground, the same elevation as the CFDC inlet. CRAFT filters were drawn for 6 hours at a flow rate of 10 L min<sup>-1</sup> at standard temperature and pressure (STP) conditions (T = 273 K, 1013.5 mb), at this site and at CSU. IS filters (0.2 μm pore size) were drawn for 6 hours at a flow rate of 13 L min<sup>-1</sup>. CFDC sampling overlapped with the IS filter period, but operating temperature was varied.

## 745 3 Results

### 3.1 Comparison of cases with perfect temporal overlap of sample data collections

Figure 1a compares IS and CFDC data for two 4-hour study periods at the CSU site. In the figure CFDC INP concentrations at -16°C are integrated and averaged for the entire IS filter sampling period for comparison to IS data collected both on filters and using the BioSampler. *Considering the capture efficiencies versus size noted in Section 2.2, the lack of significant difference in IS  $n_{INPs}(T)$  measured with the filters of 0.2 and 3 μm pore sizes implies that most INPs were likely large enough to be captured effectively. This crudely suggests an INP mode size at about 1 μm or larger. This is also a size that is collected with high efficiency in the Biosampler, for which similar INP concentrations were measured.* This example also shows the uncertainties in temperature spectra of INP number concentration from the IS. In this case, one can see a range of about a 4 factor in INP number concentration and an equivalent range of 2 to 4°C using different collection methods, and in consideration of confidence in measurements made at any particular temperature. The CFDC data collected using the aerosol concentrator are in agreement within uncertainties of all particle collection methods in this case.

In Fig. 1b, results are shown from a case where filter rinse suspension and BioSampler suspension were also shared with the CS instrument for offline processing of samples collected from the CSU site on September 6, 2013. There is significant overlap between the IS and CS data in the temperature range from -6 to -23°C (the lowest temperature limit of IS processing for these particular experiments). No significant bias is discernable between IS and CS data for any of the collection methods. Once again, correspondence of the CFDC data (using the aerosol concentrator in this case) with other methods is good at a processing temperature of -18.2°C. However, the CFDC data falls a factor of 2-5 lower than the immersion freezing methods. This is similar to data reported in Garcia et al. (2012) for which the discrepancy was attributed primarily to the failure of the CFDC instrument to sample larger aerosols. Nevertheless, results from this sampling day support the conclusions of general agreement between methods obtained in Fig. 1a.

Figure 2 shows results from three additional cases for which there was perfect temporal co-sampling by the CFDC, IS, CS and MOUDI-DFT methods. In these cases, the IS and CS shared samples of particles collected during the same time period, while the MOUDI-DFT was operated independently. We note that the error bars on MOUDI data reflect upper and lower bound estimates, as discussed in section 2.1.3. Figure 2 highlights some points already made, but also the occurrence of a range of discrepancies in  $n_{INPs}(T)$  between the MOUDI-DFT and other methods, and for CFDC data collected simultaneously at temperatures below -20°C. The CS method typically measures the highest  $n_{INPs}(T)$  overall for the same collections of aerosols (filter or BioSampler), suggesting a temperature offset of at least 1°C between these systems that may have as its source the temperature measurement of the liquid wells or

780 drops. The MOUDI-DFT results trend with the other immersion freezing methods on all days, but agree quantitatively with them on only one of three days (Fig. 2a) and fall lower than  $n_{INPs}(T)$  determined by the CS and IS on two other days; by a factor of 2 to 5 (Fig. 2c) in one case and 20 to 50 in the other (Fig. 2b). These two cases have been discussed previously in Mason et al. (2015), and we will revisit the largest discrepancies in both cases in later discussion. Similar to the MOUDI-DFT results, the CFDC data also show a consistent underestimate of  $n_{INPs}(T)$  compared to the CS and IS in all three cases, with a trend that increases from a factor of 2-4 at  $-23^{\circ}\text{C}$ , up to 10 times at  $-30^{\circ}\text{C}$  (Fig. 2a).

### 3.2 Comparison for cases of imperfect temporal overlap of sample data collections

785 The data shown in Fig. 1 and Fig. 2, for which there was complete temporal overlap of observations, provide a limited number of evaluations of measurement correspondence and uncertainties that may occur due to different size ranges of collection and natural variations in INP compositions and concentrations that may occur over varied sampling times as measured across the mixed-phase cloud temperature regime. This situation will surely be improved in future studies as many different instrument teams worldwide begin to compare data collected at common sites. To expand understanding, we considered all cases in which the CFDC was sampling simultaneously  
790 with other methods, but without the restriction of a single CFDC processing temperature for the full sampling period. There are also cases when the offline sample periods overlapped but did not perfectly align. Thus, while seeking further insights by folding in data from additional times and collection sites, we must acknowledge that such comparisons leave open the possibility that temporal variability may impact comparison of methods. Nevertheless, this replicates many field study situations where multiple ice nucleating instruments may be deployed, but may not  
795 sample for the same time periods.

In Fig. 3, we combine periods of perfect sampling overlap with these other cases for which one or more of the immersion freezing methods were performed for a few-hour period, during which CFDC sampling intervals (typically 10-15 minutes at a single temperature) occurred. Comparison of the CFDC and IS measurements are shown in Fig. 3a. These results reinforce those in Fig. 2, indicating that the IS assessment of  $n_{INPs}(T)$  agrees on  
800 average with the CFDC-measured values when the CFDC processed particles at 105% RH at the lower end of the dynamic range of  $n_{INPs}(T)$ . The IS method, however, measures higher concentrations than the CFDC at higher  $n_{INPs}(T)$ , resulting in a non-unity relational slope. The linear relational slope between IS and CFDC data shown by the light gray dashed line in Fig. 3a. The same representation is applied in all panels of Fig. 3. We provide these fits only to show general trends between the different data sets and do not provide fit parameters herein because a deeper  
805 consideration of the source of discrepancies requires additional inspection of trends as a function of temperature, which follows below. Higher  $n_{INPs}(T)$  typically occur at lower temperatures. Results are similar regardless of measurement site, but with relatively high variability in the relation between single CFDC and IS measurements even at a single site, and with greater discrepancy in the data set from Colby, KS, which we suggest is the result of an abundance of larger INPs not sampled by the CFDC during this harvesting period.

810 The MOUDI-DFT data show the best correspondence overall versus the CFDC measurements (Fig. 3b), irrespective of whether all aerosol sizes are considered for the DFT measurement or are limited to a range of particle

sizes similar to those entering the CFDC. There is a slight positive bias for the MOUDI-DFT method when all sizes are considered, as expected given the CFDC limitation on particle sizes sampled.

815 Overlapping comparisons between the CS and CFDC, and CRAFT and CFDC, while more limited (Fig. 3c), show a relatively high bias of the CS and CRAFT data, most exaggerated at higher  $n_{INPs}(T)$  and correlated with lower temperatures as discussed shortly.

820 Overall comparisons by offline method versus the CFDC are shown in Fig. 3d. These demonstrate that although a consistent linear (but not 1:1) relationship could be inferred between offline immersion freezing and CFDC measurements, discrepancies for all methods and sampling times taken together at a CFDC  $n_{INP}(T)$  of  $1 \text{ L}^{-1}$  can reach nearly two orders of magnitude. Discrepancies appear to reduce to within about 1 order of magnitude at higher  $n_{INPs}(T)$ , although the degree to which this is real or the result of a fewer number of cases is not yet clear. We may note of course that CFDC measurements have their greatest uncertainties in the range of concentrations at or below  $1 \text{ L}^{-1}$ .

825 The same data sets used in Fig. 3, and compiled in SI Table 1, are used in Fig. 4 to explore the temperature dependence of immersion freezing measurement results versus the CFDC when all sampling scenarios are considered (multiple aerosol scenarios, perfect or imperfect overlap of sampling times). In examining the IS versus CFDC comparisons (Fig. 4a), the scatter in the relation is again the most striking feature, while the temperature-dependent bias also becomes clear to a greater or lesser degree at all sampling sites, the least at CSU and the SGP site, and the most at Bodega Bay and in the harvesting period in Kansas. The strong positive bias of INP measurements by the IS at lower temperatures in Kansas is not consistent with the fact that larger INPs ( $>2.5 \mu\text{m}$ ), that are not sampled by the CFDC, are not thought to dominate INPs at lower temperatures (Mason et al., 2016). A more modest positive temperature bias is noted in comparing MOUDI and CFDC concentrations versus temperature at below  $-25\text{C}$  (Fig. 4b), and the underestimate of INP concentrations due to the elimination of coarse mode aerosols in CFDC sampling ranges from about 2 to 4 times (see MOUDI “all” versus “size” in Fig. 4b), consistent with the estimates of coarse mode INP fractions by Mason et al. (2016). We may note similarly good agreement between INP concentrations measured by the CFDC and DFT methods across similar temperature ranges for marine aerosols (DeMott et al., 2016). Strong positive biases of CS and CRAFT measured INP concentrations versus the CFDC measurements are seen to progressively occur as temperatures decrease from  $-20$  to  $-30\text{C}$  (Fig. 4c).

#### 4 Discussion

840 In this section, we summarize observations regarding comparisons of the INP measurement methods and discuss potential reasons for discrepancies that bear future investigation. It has been shown that there are times when multiple measurement techniques give excellent agreement for  $n_{INPs}(T)$  in the immersion freezing mode. Agreement is best at temperatures warmer than  $-20\text{C}$  and for  $n_{INPs}(T)$  less than  $\sim 5 \text{ L}^{-1}$ . At lower temperatures and higher  $n_{INPs}(T)$ , most offline immersion freezing methods, with the exception of MOUDI-DFT, estimate higher than the online CFDC method, by ratios ranging from a few to 10 times. We must caution that the overall range of  $n_{INPs}(T)$  assessed and values present at different temperatures may reflect the aerosol measured at ground level at the selected sites

and times, scenarios that may not represent all locations and times worldwide. Nor may these results be the same if the comparisons were made entirely for free tropospheric aerosols, for example as assessed from an aircraft or at some mountaintop sites. Nevertheless, the potential issues in obtaining agreement between methods will be common in any sampling scenario.

A factor in any series of immersion freezing measurements is the time dependence of nucleation. In a study of the time-dependent freezing of kaolinite particles, Welti et al. (2012) demonstrated that the majority of freezing occurred within about a period of 10 s or less at the temperatures -30 to -37°C, with 0.8 µm diameter particles needing far less time for activation than 0.4 µm particles. Studies of freezing rates for other natural INP types across broader temperature ranges indicate that immersion freezing is indeed not a purely stochastic process and is far more sensitive to temperature, with the consequence that the increase in  $n_{INPs}(T)$  achieved when droplets remain at a single temperature for periods longer than seconds to minutes are typically overcome by a few degrees of additional cooling (Vali, 2014; Wright et al. 2013). The CFDC  $n_{INPs}(T)$  attributed here to immersion freezing were obtained for a total processing time of approximately 7 s, the last 2 s of which activated droplets are evaporating (DeMott et al., 2015). This residence time is constrained by flow rates required for limiting thermally-driven reverse flow circulations in the CFDC. By comparison to the Welti et al. (2012) study, it seems likely that the CFDC activation times allow for capturing the majority of immersion freezing activity in most circumstances. Nevertheless, we expect that the CFDC might underestimate  $n_{INPs}(T)$  to a greater extent than the IS measurements, which are made while ramping at a very slow cooling rate equivalent to 1°C in 3 minutes. Since the DFT uses much faster cooling rates (5 - 10°C min<sup>-1</sup>), this might explain the better correspondence with the CFDC data. However, it cannot explain the temperature-dependent nature of the bias between other immersion freezing methods and the CFDC, and so seems not the only source of this discrepancy.

Here we must also reiterate that the processing of submicron mode mineral dust particles at 105% RH in the CFDC has been shown to underestimate  $n_{INPs}(T)$  by an average, temperature-independent factor of 3 times, as confirmed by laboratory cloud chamber simulations. This factor was related to the fact that higher RH is typically required to fully activate all particles (hygroscopic or hydrophobic) as droplets to subsequently be available for freezing in the CFDC residence time (DeMott et al., 2015; Garimella et al., 2017). However, practical operation of the CFDC at higher RH (109% may be required for full activation) is prohibited in sampling of natural aerosol distributions because the largest aerosols could persist as droplets through the evaporation section of the instrument under these conditions, thus contaminating INP determination using optical sizing. Hence, it is unknown if natural INP populations are being underestimated for similar reasons. Based on the recent study of Garimella et al. (2017), it seems possible that underestimation of INP concentrations occurs for CFDC-style instruments independent of the aerosol type. Consequently, lines indicating a factor of 3 higher than the 1:1 relation have been placed on plots in the panels of Fig. 3. While it is noted that increasing the CFDC  $n_{INPs}(T)$  by 3 times leads to better overall agreement of CFDC data with the CS and CRAFT data especially, this constant expected offset does not explain the progressive underestimate of the CFDC in comparison to most immersion freezing methods (the IS, CS and CRAFT being most like other methods used worldwide) at higher  $n_{INPs}(T)$  and lower temperatures.

A factor that could artificially increase  $n_{INPs}(T)$  at lower temperatures in methods that immerse the entire aerosol population first into liquid (IS, CS, CRAFT) is the potential breakup of aggregates containing multiple INPs (e.g.,  
885 via the deflocculation of small aggregates as a result of the strong reduction in di- and trivalent cation concentrations in the deionized water used for making dilution series, or by the fragmentation of mucigels (Hill et al., 2016)) and the possible dissolution release of surface-active INP materials present on single particles when suspended in deionized water (O'Sullivan et al., 2016). It seems possible that such action would have the greatest impact on INPs active at lower temperatures (rather than the most active INPs), since these may be small clay/organic matter  
890 aggregates or flocs that fragment when exposed to deionized water. Since the MOUDI-DFT method immerses a relatively small number of particles directly and without agitation in small drops prior to freezing, it is interesting to note that the least temperature-dependent bias occurs for these measurements in comparison to the CFDC. This point is shown more clearly by comparing only the offline immersion freezing methods in Fig. 5. In this figure, the different measured INP concentrations are taken as a ratio versus the IS, which sampled the most times and scenarios. Data at one degree temperature resolution are included in this comparison, as compiled in Table S2.  
895 Again, relatively high variability of at least 1 order of magnitude at any temperature is noted for the relations between methods. Among methods that involve immersion of all particles in a single volume of water prior to setting up arrays (CS, CRAFT, IS), the IS falls to the low side of the other measurements by an average factor of about 2.5. This is not a significant difference, in consideration of the likely temperature uncertainties discussed in relation to Figures 1 and 2. The MOUDI-DFT method that immerses relatively small populations of particles, shows relative equivalence to the full immersion methods at modest to moderately supercooled temperatures, but measured consistently lower INP concentrations at below about  $-20^{\circ}\text{C}$  in the few cases when co-sampling was conducted with the IS (CSU and Kansas). This is consistent with the discrepancy seen also versus CFDC data. Interestingly, a lower temperature enhancement of INPs appearing in full immersion methods versus continuous flow methods was not  
900 observed in recent laboratory tests comparing many measurement methods while sampling mineral, soil dust and biological particle samples that had been purposely limited to sizes smaller than  $2\ \mu\text{m}$  (DeMott et al., 2017). While this points to coarse mode particles and their dissolution/fragmentation into multiple INP units as the source of differences, future experiments will be needed to confirm or deny that this is either an artifact or a behavior in natural aerosols that the CFDC cannot effectively capture.

910 Particle size limitations lead to CFDC underestimates of  $n_{INPs}(T)$  in comparison to some immersion freezing methods. This is because of the need to remove particles larger than  $2.4\ \mu\text{m}$ . This removal of larger aerosols is necessary when differentiating grown ice crystals from aerosols by size alone. Even absent the use of impactors, it would be difficult for most online systems to effectively sample larger particles due to the design of inlet systems. With reference to the study of Mason et al. (2016), which entailed sampling with the MOUDI-DFT method at various sites, one might estimate that on average about 50% of INPs are at sizes larger than  $2.4\ \mu\text{m}$  in the surface  
915 boundary layer. Comparison of MOUDI-DFT with CFDC data in this study is consistent with this same estimate (Fig. 3b). Again, this would not apparently explain a progressive slight increase in CFDC underestimation versus the MOUDI-DFT at lower temperatures unless larger INPs specially dominate ice nucleation at lower temperatures, a result not consistent with Mason et al. (2016).

920 In evaluating the low temperature discrepancies by noting the better correspondence of MOUDI-DFT and CFDC  
methods, it is also necessary to note the potential issue of particle bounce in the MOUDI in some cases (Mason et  
al., 2016). While the conditions for this to occur are not well quantified, since both INP size and phase state (as this  
may be influenced by low relative humidity) may affect bounce, very dry conditions have been indicated as times  
when this may become an issue for MOUDI impaction onto the substrates used in the DFT instrument. Interestingly,  
925 average RH during the sampling period on November 13, 2013 (Fig. 2b) was between 15-20% during the sampling  
period versus 40-45% for days on either side (Figs. 2a, c), potentially impacting and explaining the MOUDI-DFT  
results on this day. For this reason, this day was excluded in Fig. 3 to Fig. 5. Sample humidification of the system  
could mitigate this factor as a potential issue in future sampling.

## 5 Conclusions

930 This study has inspected the correspondence of ice nucleation measurement systems for co-sampling ambient ice  
nucleating particles. In this case, we considered systems for measuring immersion freezing nucleation with a  
common online method used in a manner to induce activation of cloud droplets prior to ice nucleation. [Very good  
agreement within uncertainty limits was obtained under](#) many conditions for samples that had perfect temporal  
overlap. In other cases, discrepancies can approach two orders of magnitude and are not explicable without inferring  
935 systematic artefacts inherent to one or more techniques. The results summarized in Fig. 3d show the uncertainties  
that can be expected when employing one or more of these instrument systems for measuring atmospheric INPs.  
Within these uncertainties, the data suggest that the low bias of immersion freezing methods reported by Hiranuma  
et al. (2015) for sampling of individual surrogate dusts in the laboratory was not evident in these ambient data sets.

940 With regard to particle sampling methods for immersion freezing measurements, use of a BioSampler or a filter  
was interchangeable, at least for the continental boundary layer sampling for which these methods were compared.  
This was demonstrated for individual and for cross-technique methods (IS versus CS) for assessing immersion  
freezing from the same samples. Since Nuclepore filters seem to efficiently capture and release INPs, these provide  
ease of use benefits in many field scenarios, although the role of retention of particles on some filter types has not  
been assessed here. [Potential effects of sample storage protocol also remain to be investigated.](#)

945 The strongest discrepancies between methods appear at both warmer and colder ends of the scale of mixed-phase  
cloud freezing temperatures. At the warmer end ( $T > -20^{\circ}\text{C}$ ), sampling statistics and uncertainties can dominate  
comparisons of online and offline methods. Full explanations for the maximum 2 orders of magnitude range of  
variation in this temperature regime remains unresolved. In contrast, at lower temperatures the IS, CS and CRAFT  
methods measured more INPs than detected by the CFDC and MOUDI-DFT. Potential artifacts or biases are present  
950 in these comparisons and have been discussed here, including varied assessment of time dependence of ice  
nucleation, necessary exclusion of larger INPs by online instruments such as the CFDC, and immersion of all  
particles into relatively large volumes of deionized water in most, but not all, immersion freezing methods versus  
activation of single particles in CFDCs. In addition, it is expected that all CFDC type instrument data may require  
correction for not being able to access full immersion of particles until higher RH than can commonly be used when  
955 sampling ambient particles, or else this issue requires future mitigation (e.g., insertion of particles into the

instrument lamina could be improved). Hence, no assured conclusions regarding the sources of discrepancies can be stated at this time except that size biases in sampling need to be acknowledged. Effort thus remains to make INP measurements fully quantitative and comparative across methods, if correspondence within less than one order of magnitude is desired. Even amongst standard immersion freezing methods, uncertainties of a factor of a few  $n_{INPs}$  (960  $T$ ) and 2 to 4°C are likely common on the basis of this study, and may be the best that can be achieved. Application of size selection to immersion freezing collections for comparison to MOUDI-DFT data (especially at lower temperatures) and CFDC data, information on INP compositions inferred under all sampling scenarios to help constrain influences of various types (e.g., methods of Hill et al., 2016), and an inter-comparison of all methods versus a cloud parcel simulation chamber, considered as a *de facto* standard, would all assist resolution and (965 improvement of understanding of measurement discrepancies.

*Data availability.* The data used are listed in the references, tables, Supplement, and in a digital repository at CSU (<https://dspace.library.colostate.edu>).

*Competing interests.* The authors declare no competing interests.

*Acknowledgments.* Funding for this work was provided by National Science foundation grants AGS1358495 (P. J. DeMott, T. C. J. Hill, K. J. Suski, and E. J. T. Levin), AGS1010851 (M. D. Petters and J. D. Hader) and AGS1450690 (M. D. Petters, N. Rothfuss, and H. Taylor), AGS1450760 (P. J. DeMott, T. C. J. Hill, C. S. McCluskey, and S. M. Kreidenweis) and AGS1433517 (G. P. Schill). Support for operations at the U.S. Department of Energy Southern Great Plains site was provided by the Atmospheric Radiation Measurement (ARM) Climate Research Facility, a U.S. Department of Energy Office of Science user facility sponsored by the Office of Biological and Environmental Research. A. K. Bertram, R. H. Mason, and C. Chou acknowledge support of the Natural Sciences and Engineering Research Council of Canada. Y. Tobo acknowledges support from JSPS KAKENHI Grant Number 15K13570, 16H06020, the NIPR Project Research KP-3, and the Arctic Challenge for Sustainability (ArCS) project. Y. Boose thankfully acknowledges support from the Zeno Karl Schindler foundation. Special thanks to Kim Prather, Andrew Marin and colleagues at the University of California, San Diego for their logistical support (975 during studies at Bodega Bay. We also thank the University of California, Davis Bodega Marine Laboratory for the use of laboratory and office space and shipping and physical plant support while collecting data. We thank the National Park Service and Prof. Jeffrey Collett for use of their respective mobile laboratories during various field study deployments. We thank Freddie Lamm, Dan Foster, and Marv Farmer at the KSU NW Research Center for their help with coordinating the measurements. Finally, we thank the Nature Conservancy's Canyonlands Research (980 Center and Field Station Manager Philip Adams for helping arrange and select sites for measurements there.

## References

- Beall, C. M., Stokes, M. D., Hill, T. C., DeMott, P. J., DeWald, J. T., and Prather, K. A.: Automation and Heat Transfer Characterization of Immersion Mode Spectroscopy for Analysis of Ice Nucleating Particles, *Atmos. Meas. Tech. Discuss.*, doi:10.5194/amt-2016-412, in review, 2017.
- 990 Boose, Y., Sierau, B., García, M. I., Rodríguez, S., Alastuey, A., Linke, C., Schnaiter, M., Kupiszewski, P., Kanji, Z. A., and Lohmann, U.: Ice nucleating particles in the Saharan Air Layer, *Atmos. Chem. Phys.*, 16, 9067-9087, doi:10.5194/acp-16-9067-2016, 2016.
- DeMott et al., Overview of results from the Fifth International Workshop on Ice Nucleation part 2 (FIN-02): Laboratory intercomparisons of ice nucleation measurements, In preparation for submission to *Atmos. Chem. Phys.*, 2017.
- 995 DeMott, P. J., Prenni, A. J., Liu, X., Kreidenweis, S. M., Petters, M. D., Twohy, C. H., Richardson, M. S., Eidhammer, T., and Rogers, D. C.: Predicting global atmospheric ice nuclei distributions and their impacts on climate, *Proc. Natnl. Acad. Sci.*, 107 (25), 11217-11222, 2010.
- DeMott, P. J., Prenni, A. J., McMeeking, G. R., Sullivan, R. C., Petters, M. D., Tobo, Y., Niemand, M., Möhler, O., Snider, J. R., Wang, Z., and Kreidenweis, S. M.: Integrating laboratory and field data to quantify the immersion freezing ice nucleation activity of mineral dust particles, *Atmos. Chem. Phys.*, 15, 393-409, doi:10.5194/acp-15-393-2015, 2015.
- 1000 DeMott, P. J., T. C. J. Hill, C. S. McCluskey, K. A. Prather, D. B. Collins, R. C. Sullivan, M. J. Ruppel, R. H. Mason, V. E. Irish, T. Lee, C. Y. Hwang, T. S. Rhee, J. R. Snider, G. R. McMeeking, S. Dhaniyala, E. R. Lewis, J. J. B. Wentzell, J. Abbatt, C. Lee, C. M. Sultana, A. P. Ault, J. L. Axson, M. Diaz Martinez, I. Venero, G. Santos-Figueroa, M. D. Stokes, G. B. Deane, O. L. Mayol-Bracero, V. H. Grassian, T. H. Bertram, A. K. Bertram, B. F. Moffett, and G. D. Franc: Sea spray aerosol as a unique source of ice nucleating particles. *Proc. Natnl. Acad. Sci.*, 113 (21), 5797-, doi:10.1073/pnas.1514034112, 2016.
- 1005 Eidhammer, T., DeMott, P. J., Prenni, A. J., Petters, M. D., Twohy, C. H., Rogers, D. C., Stith, J., Heymsfield, A., Wang, Z., Haimov, S., French, J., Pratt, K., Prather, K., Murphy, S., Seinfeld, J., Subramanian, R., and Kreidenweis, S. M.: Ice initiation by aerosol particles: Measured and predicted ice nuclei concentrations versus measured ice crystal concentrations in an orographic wave cloud, *J. Atmos. Sci.*, 67, 2417-2436, doi:10.1175/2010JAS3266.1, 2010.
- Emersic, C., Connolly, P. J., Boulton, S., Campana, M., and Li, Z.: Investigating the discrepancy between wet-suspension- and dry-dispersion-derived ice nucleation efficiency of mineral particles, *Atmos. Chem. Phys.*, 15, 11311-11326, doi:10.5194/acp-15-11311-2015, 2015.
- 1015 Garcia, E., Hill, T. C. J., Prenni, A. J., DeMott, P. J., Franc, G. D., and Kreidenweis, S. M.: Biogenic ice nuclei in boundary layer air over two U.S. High Plains agricultural regions, *J. Geophys. Res.*, 117, D18209, doi:10.1029/2012JD018343, 2012.
- 1020 Garimella, S., Rothenberg, D. A., Wolf, M. J., David, R. O., Kanji, Z. A., Wang, C., Roesch, M., and Cziczo, D. J.: Uncertainty in counting ice nucleating particles with continuous diffusion flow chambers, *Atmos. Chem. Phys. Discuss.*, doi:10.5194/acp-2016-1180, in review, 2017.

- Grawe, S., Augustin-Bauditz, S., Hartmann, S., Hellner, L., Pettersson, J. B. C., Prager, A., Stratmann, F., and Wex, H.: The immersion freezing behavior of ash particles from wood and brown coal burning, *Atmos. Chem. Phys.*, 16, 13911-13928, doi:10.5194/acp-16-13911-2016, 2016.
- 1025 Hader, J. D., Wright, T. P., and Petters, M. D.: Contribution of pollen to atmospheric ice nuclei concentrations, *Atmos. Chem. Phys.*, 14, 5433-5449, doi:10.5194/acp-14-5433-2014, 2014.
- Hill, T. C. J., Moffett, B. F., DeMott, P. J., Georgakopoulos, D. G., Stump, W. L., and Franc, G. D.: Measurement of ice nucleation-active bacteria on plants and in precipitation by quantitative PCR. *Appl. Environ. Microbiol.* 80(4):1256-1267, doi: 10.1128/AEM.02967-13, 2014.
- 1030 Hill, T. C. J., P. J. DeMott, Y. Tobo, J. Fröhlich-Nowoisky, B. F. Moffett, G. D. Franc, and S. M. Kreidenweis: Sources of organic ice nucleating particles in soils, *Atmos. Chem. Phys.*, 16, 7195–7211, doi:10.5194/acp-2016-1, 2016.
- Hiranuma, N., Augustin-Bauditz, S., Bingemer, H., Budke, C., Curtius, J., Danielczok, A., Diehl, K., Dreischmeier, K., Ebert, M., Frank, F., Hoffmann, N., Kandler, K., Kiselev, A., Koop, T., Leisner, T., Möhler, O., Nillius, B., Peckhaus, A., Rose, D., Weinbruch, S., Wex, H., Boose, Y., DeMott, P. J., Hader, J. D., Hill, T. C. J., Kanji, Z. A., Kulkarni, G., Levin, E. J. T., McCluskey, C. S., Murakami, M., Murray, B. J., Niedermeier, D., Petters, M. D., O'Sullivan, D., Saito, A., Schill, G. P., Tajiri, T., Tolbert, M. A., Welti, A., Whale, T. F., Wright, T. P., and Yamashita, K.: A comprehensive laboratory study on the immersion freezing behavior of illite NX particles: a comparison of 17 ice nucleation measurement techniques, *Atmos. Chem. Phys.*, 15, 2489-2518, doi:10.5194/acp-15-2489-2015, 2015.
- 1035 Huffman, J. A., Prenni, A. J., DeMott, P. J., Pöhlker, C., Mason, R. H., Robinson, N. H., Fröhlich-Nowoisky, J., Tobo, Y., Després, V. R., Garcia, E., Gochis, D. J., Harris, E., Müller-Germann, I., Ruzene, C., Schmer, B., Sinha, B., Day, D. A., Andreae, M. O., Jimenez, J. L., Gallagher, M., Kreidenweis, S. M., Bertram, A. K., and Pöschl, U.: High concentrations of biological aerosol particles and ice nuclei during and after rain, *Atmos. Chem. Phys.*, 13, 6151-6164, doi:10.5194/acp-13-6151-2013, 2013.
- 1045 Koop, T., Luo, B., Biermann, U. M., Crutzen, P. J., and Peter, T.: Freezing of HNO<sub>3</sub> / H<sub>2</sub>SO<sub>4</sub> / H<sub>2</sub>O solutions at stratospheric temperatures: Nucleation statistics and experiments, *J. Phys. Chem. A*, 101, 1117–1133, doi:10.1021/jp9626531, 1997.
- 1050 Martin, A. C., Cornwell, G. C., Atwood, S. A., Moore, K. A., Rothfuss, N. E., Taylor, H., DeMott, P. J., Kreidenweis, S. M., Petters, M. D., and Prather, K. A.: Transport of pollution to a remote coastal site during gap flow from California's interior: impacts on aerosol composition, clouds, and radiative balance, *Atmos. Chem. Phys.*, 17, 1491-1509, doi:10.5194/acp-17-1491-2017, 2017.
- 1055 Mason, R. H., C. Chou, C. S. McCluskey, E. J. T. Levin, C. L. Schiller, T. C. J. Hill, J. A. Huffman, P. J. DeMott, and A. K. Bertram: The micro-orifice uniform deposit impactor-droplet freezing technique (MOUDI-DFT) for measuring concentrations of ice nucleating particles as a function of size: improvements and initial validation, *Atmos. Meas. Tech.*, 8, 2449–2462, 2015.
- Mason, R. H., Si, M., Chou, C., Irish, V. E., Dickie, R., Elizondo, P., Wong, R., Brintnell, M., Elsasser, M., Lassar, W. M., Pierce, K. M., Leitch, W. R., MacDonald, A. M., Platt, A., Toom-Sauntry, D., Sarda-Estève, R.,

- 1060 Schiller, C. L., Suski, K. J., Hill, T. C. J., Abbatt, J. P. D., Huffman, J. A., DeMott, P. J., and Bertram, A. K.: Size-resolved measurements of ice-nucleating particles at six locations in North America and one in Europe, *Atmos. Chem. Phys.*, 16, 1637-1651, doi:10.5194/acp-16-1637-2016, 2016.
- McCluskey, C. S., DeMott, P. J., Prenni, A. J., Levin, E. J., McMeeking, G. R., Sullivan, A. P., Hill, T. C., Nakao, S., Carrico, C. M., and Kreidenweis, S. M.: Characteristics of atmospheric ice nucleating particles associated with biomass burning in the US: Prescribed burns and wildfires, *J. Geophys. Res.*, 119, 10458–10470, 2014.
- 1065 Murray, B. J., O’Sullivan, D., Atkinson, J. D., and Webb, M. E.: Ice nucleation by particles immersed in supercooled cloud droplets, *Chem. Soc. Rev.*, 41, 6519–6554, 2012.
- Ortega, J., Turnipseed, A., Guenther, A. B., Karl, T. G., Day, D. A., Gochis, D., Huffman, J. A., Prenni, A. J., Levin, E. J. T., Kreidenweis, S. M., DeMott, P. J., Tobo, Y., Patton, E. G., Hodzic, A., Cui, Y. Y., Harley, P. C.,
- 1070 Hornbrook, R. S., Apel, E. C., Monson, R. K., Eller, A. S. D., Greenberg, J. P., Barth, M. C., Campuzano-Jost, P., Palm, B. B., Jimenez, J. L., Aiken, A. C., Dubey, M. K., Geron, C., Offenberg, J., Ryan, M. G., Fornwalt, P. J., Pryor, S. C., Keutsch, F. N., DiGangi, J. P., Chan, A. W. H., Goldstein, A. H., Wolfe, G. M., Kim, S., Kaser, L., Schnitzhofer, R., Hansel, A., Cantrell, C. A., Mauldin, R. L., and Smith, J. N.: Overview of the Manitou Experimental Forest Observatory: site description and selected science results from 2008 to 2013, *Atmos. Chem. Phys.*, 14, 6345-6367, doi:10.5194/acp-14-6345-2014, 2014.
- 1075 O’Sullivan, D., Murray, B. J., Ross, J. F., and Webb, M. E.: The adsorption of fungal ice-nucleating proteins on mineral dusts: a terrestrial reservoir of atmospheric ice-nucleating particles, *Atmos. Chem. Phys.*, 16, 7879-7887, doi:10.5194/acp-16-7879-2016, 2016.
- Petters, M. D., Parsons, M. T., Prenni, A. J., DeMott, P. J., Kreidenweis, S. M., Carrico, C. M., Sullivan, A. P.,
- 1080 McMeeking, G. R., Levin, E., Wold, C. E., Collett, J. L. J., and Moosmüller, H.: Ice nuclei emissions from biomass burning, *J. Geophys. Res.*, 114, D07209, doi:10.1029/2008JD011532, 2009.
- Petters, M. D. and Wright, T. P.: Revisiting ice nucleation from precipitation samples, *Geophys. Res. Lett.*, 42, 8758–8766, 2015.
- Prenni, A. J., Tobo, Y., Garcia, E., DeMott, P. J., McCluskey, C., Kreidenweis, S. M., Prenni, J., Huffman, A.,
- 1085 Pöschl, U., and Pöhlker, C.: The impact of rain on ice nuclei populations. *Geophys. Res. Lett.*, 40, doi:10.1029/2012GL053953, 2013.
- Prenni A. J., DeMott, P. J., Rogers, D. C., Kreidenweis, S. M., McFarquhar, G. M., Zhang, G., and Poellot, M. R.: Ice nuclei characteristics from M-PACE and their relation to ice formation in clouds. *Tellus* 61B(2):436–448, 2009.
- 1090 Ralph, F. M., Prather, K. A., Cayan, D., Spackman, J. R., DeMott, P. J., Dettinger, M., Fairall, C., Leung, R., Rosenfeld, D., Rutledge, S., Waliser, D., White, A. B., Cordeira, J., Martin, A., Helly, J., and Intrieri, J.: CalWater Field Studies Designed to Quantify the Roles of Atmospheric Rivers and Aerosols in Modulating U.S. West Coast Precipitation in a Changing Climate. *Bull. Amer. Meteor. Soc.*, 97, 1209–1228, doi: 10.1175/BAMS-D-14-00043.1, 2016.

- 1095 Schill, G. P., S. H. Jathar, J. K. Krodos, E. J. T. Levin, A. M. Galang, B. Friedman, D. K. Farmer, J. R. Pierce, S. M. Kreidenweis, and P. J. DeMott, 2016: Ice nucleating particle emissions from photo-chemically-aged diesel and biodiesel exhaust, *Geophys. Res. Lett.*, doi: 10.1002/2016GL069529.
- Schrod, J., Danielczok, A., Weber, D., Ebert, M., Thomson, E. S., and Bingemer, H. G.: Re-evaluating the Frankfurt isothermal static diffusion chamber for ice nucleation, *Atmos. Meas. Tech.*, 9, 1313-1324, doi:10.5194/amt-9-1313-2016, 2016a.
- 1100 Schrod, J., Weber, D., Drücke, J., Keleshis, C., Pikridas, M., Ebert, M., Cvetkovic, B., Nickovic, S., Marinou, E., Baars, H., Vrekoussis, M., Mihalopoulos, N., Sciare, J., Curtius, J., and Bingemer, H. G.: Ice nucleating particles over the Eastern Mediterranean measured by unmanned aircraft systems, *Atmos. Chem. Phys. Discuss.*, doi:10.5194/acp-2016-1098, in review, 2016b.
- 1105 Spurny K. R., and Lodge, J. P., Jr.: Collection efficiency tables—for membrane filters used in the sampling and analysis of aerosols and hydrosols. *NCAR Technical Note* (National Center for Atmospheric Research, Boulder, CO), NCAR-TN/STR-77, Vol I, 1972.
- Stopelli, E., Conen, F., Morris, C. E., Herrmann, E., Bukowiecki, N., and Alewell, C.: Ice nucleation active particles are efficiently removed by precipitating clouds, *Scientific Reports* 5:16433, DOI: 10.1038/srep16433, 2015.
- 1110 Tobo, Y.: An improved approach for measuring immersion freezing in large droplets over a wide temperature range, *Scientific Reports*, 6:32930, doi: 10.1038/srep32930, 2016.
- Tobo, Y., Prenni, A.J., DeMott, P.J., Huffman, J.A., McCluskey, C.S., Tian, G., Pöhlker, C., Pöschl, U., Kreidenweis, S.M., 2013: Biological aerosol particles as a key determinant of ice nuclei populations in a forest ecosystem. *J. Geophys. Res. -Atmos.*, 118, 10100-10110, doi:10.1002/jgrd.50801, 2013.
- 1115 Vali, G.: Quantitative evaluation of experimental results on the heterogeneous freezing nucleation of supercooled liquids, *J. Atmos. Sci.*, 28, 402–409, 1971.
- Vali, G.: Interpretation of freezing nucleation experiments: singular and stochastic; sites and surfaces, *Atmos. Chem. Phys.*, 14, 5271–5294, doi:10.5194/acp-14-5271-2014, 2014.
- 1120 Vali, G., DeMott, P. J., Möhler, O., and Whale, T. F.: Technical Note: A proposal for ice nucleation terminology, *Atmos. Chem. Phys.*, 15, 10263-10270, doi:10.5194/acp-15-10263-2015, 2015.
- Welti, A., Lüönd, F., Kanji, Z. A., Stetzer, O., and Lohmann, U.: Time dependence of immersion freezing: an experimental study on size selected kaolinite particles, *Atmos. Chem. Phys.*, 12, 9893-9907, doi:10.5194/acp-12-9893-2012, 2012.
- 1125 Wex, H., Augustin-Bauditz, S., Boose, Y., Budke, C., Curtius, J., Diehl, K., Dreyer, A., Frank, F., Hartmann, S., Hiranuma, N., Jantsch, E., Kanji, Z. A., Kiselev, A., Koop, T., Möhler, O., Niedermeier, D., Nillius, B., Rösch, M., Rose, D., Schmidt, C., Steinke, I., and Stratmann, F.: Intercomparing different devices for the investigation of ice nucleating particles using Snomax® as test substance, *Atmos. Chem. Phys.*, 15, 1463-1485, doi:10.5194/acp-15-1463-2015, 2015.
- 1130 Willeke, K., Lin, X., Grinshpun, S. A.: Improved Aerosol Collection by Combined Impaction and Centrifugal Motion, *Aerosol Science and Technology*, 28(5), 439–456. doi:10.1080/02786829808965536, 1998.

Wright, T. P., and M. D. Petters (2013), The role of time in heterogeneous freezing nucleation, *J. Geophys. Res. Atmos.*, **118**, 3731–3743, doi:10.1002/jgrd.50365.

1135 Wright, T. P., Petters, M. D., Hader, J. D., Morton, T., and Holder, A. L.: Minimal cooling rate dependence of ice nuclei activity in the immersion mode, *J. Geophys. Res. Atmos.*, 118, 10,535–10,543, doi:10.1002/jgrd.50810, 2013.

1140

1145

1150

1155

1160

**Table 1.** Samples taken during periods when the CFDC was operated at a single temperature on each date, and immersion freezing methods were aligned in time, sharing samples in some cases. Data from Waverly, CO are from Garcia et al. (2012). Sample volumes ranged from 1600 to 5500 L.

Location	Lat, Lon	Date	Elevation (m)	Standard Sample Type	Instruments
Waverly, CO	40.761, -105.076	9/29/10	1585	BioSampler	CFDC, IS
		10/4/10		BioSampler	CFDC, IS
		10/8/10		BioSampler	CFDC, IS
		11/3/10		BioSampler	CFDC, IS
CSU Atmos Chem, Fort Collins, CO	40.587, -105.150	9/6/13	1591	Ultrapure water	CFDC, IS, CS
		9/6/13		Biosampler blank	CFDC, IS, CS
		9/6/13		Biosampler	CFDC, IS, CS
		9/6/13		3 µm filter	CFDC, IS, CS
		9/6/13		0.2 µm filter	CFDC, IS, CS
		9/12/13		Biosampler	CFDC, IS
		9/12/13		3 µm filter	CFDC, IS
		9/12/13		0.2 µm filter	CFDC, IS
		11/12/13		Biosampler	CFDC, IS, CS, MOUDI-DFT
		11/12/13		3 µm filter	CFDC, IS, CS, MOUDI-DFT
		11/12/13		0.2 µm filter	CFDC, IS, CS, MOUDI-DFT
		11/13/13		Biosampler	CFDC, IS, CS, MOUDI-DFT
		11/13/13		3 µm filter	CFDC, IS, CS, MOUDI-DFT
		11/13/13		0.2 µm filter	CFDC, IS, CS, MOUDI-DFT
11/14/13	Biosampler	CFDC, IS, CS, MOUDI-DFT			

1165

1170

1175

**Table 2.** Sampling locations, elevations, dates and instruments involved in sampling at field sites when the CFDC sampled at varied temperatures during integral offline collections. All sampling at these sites were by filters, except the use of a BioSampler for the CS at Bodega Bay Marine Laboratory and the IS at Waverly, and the MOUDI-DFT at Manitou Experimental Forest (Huffman et al., 2013) and Colby (Mason et al., 2015). CFDC data from Manitou Forest are from Tobo et al. (2013). Data from Waverly, CO are from Garcia et al. (2012).

<b>Region</b>	<b>Location</b>	<b>Lat, Lon</b>	<b>Date</b>	<b>Elevation (m)</b>	<b>Instruments</b>
Forest	Manitou Experimental Forest Observatory, CO	39.094, -105.101	8/17/11, 8/18/11,	2370	CFDC, MOUDI-DFT
Agricultural	Waverly, CO	40.761, -105.076	9/29/10, 10/4/10, 10/8/10, 11/3/10	1585	CFDC, IS
Agricultural	Colby, KS	39.394, -101.066	10/14/14, 10/15/14	966	CFDC, IS, MOUDI-DFT
Agricultural	Lamont, OK	36.607, -97.488	4/30/14, 5/4/14, 5/5/14, 6/5/14, 6/7/14, 6/8,14	315	CFDC, IS
Coastal	Bodega Bay Marine Laboratory, CA	39.307, -123.066	1/26/15, 2/2/15	5	CFDC, IS, CS
Semi-arid	Canyonlands, UT	38.071, -109.563	5/11/16, 5/12/16	1627	CFDC, IS, CRAFT
Semi-rural	CSU Atmos Chem, Fort Collins, CO	40.587, -105.150	5/18/16, 5/19/16	1591	CFDC, IS, CRAFT

1180

1185

- 1190 **Table 3.** Acronyms and symbols (in italics) used
- A<sub>deposit</sub>*: total area of the sample deposit on the hydrophobic glass cover slip for the MOUDI-DFT method
- A<sub>DFT</sub>*: area of the sample monitored in the digital video during MOUDI-DFT freezing experiments
- AIDA: Karlsruhe Institute of Technology Aerosol Interactions and Dynamics of the Atmosphere cloud chamber
- BBY: reference to Bodega Bay, CA, USA field site located at the University of California, Davis Bodega Marine
- 1195 Laboratory
- BioSampler: shorthand for impinge device, the Bioaerosol sampler, SKC Inc.
- CFDC: Colorado State University Continuous Flow Diffusion Chamber
- C<sub>INPs(T)</sub>*: number concentration of INPs per volume of liquid
- CRAFT: National Institute of Polar Research (Japan) Cryogenic Refrigerator Applied to Freezing Test
- 1200 CRC: The Nature Conservancy’s Canyonlands Research Center, adjacent to Canyonlands National Park, UT, USA
- CS: North Carolina State University Cold Stage freezing assay
- CSU: Colorado State University, also used to denote the sampling site outside of the Department of Atmospheric Science’s Atmospheric Chemistry (Atmos Chem) building
- D<sub>p</sub>*: aerosol particle diameter
- 1205 *f<sub>nc</sub>*: correction factor to account for the uncertainty associated with the number of nucleation events in each experiment
- f<sub>nu</sub>*: correction factor to account for non-uniformity in particle concentration across each MOUDI sample
- INP(s): ice nucleating particle(s)
- IS: Colorado State University Ice Spectrometer
- 1210 Kansas: refers to state of Kansas sampling, at Colby, KS, USA
- LACIS: Leibniz Institute for Tropospheric Research’s Leipzig Aerosol Cloud Interaction Simulator
- MEFO: Manitou Experimental Forest Observatory
- MOUDI-DFT: University of British Columbia’s Micro-Orifice Uniform Deposit Impactor – Droplet Freezing Technique
- 1215 *n<sub>INPs(T)</sub>*: number concentration of INPs per volume of air [at a given temperature](#)
- n<sub>u</sub>*: number of drops unfrozen in immersion freezing arrays
- N*: total number of droplets or liquid entities (in arrays or condensed) in immersion freezing devices
- NoCO: Northern Colorado, referring to agricultural sampling region in Waverly, CO
- SGP: U.S. Department of Energy, Atmospheric Radiation Measurements program Southern Great Plains site,
- 1220 located near Lamont, OK, USA
- STP: standard temperature (273 K) and pressure (1013.5 mb) conditions, typically to refer to volumes converted to these conditions
- T*: Temperature (°C)
- V*: volume of individual droplets or aliquots in immersion freezing array
- 1225 *V<sub>s</sub>*: sample volume of air collected (L<sup>-1</sup>)
- V<sub>w</sub>*: total liquid volume into which particles are placed (mL)

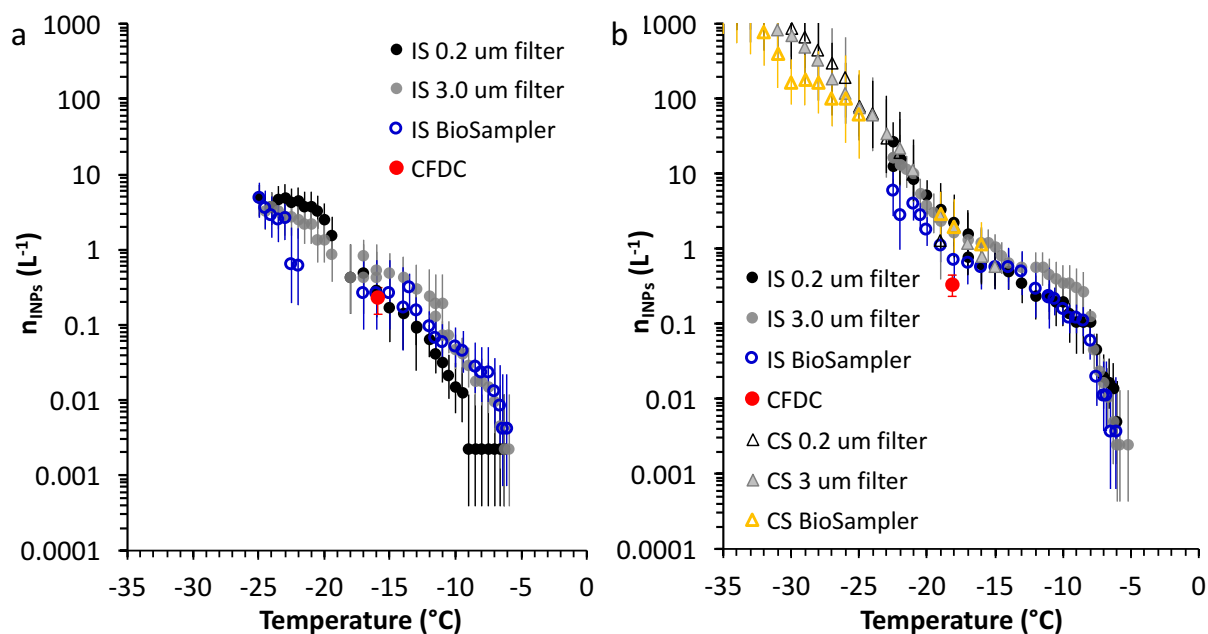
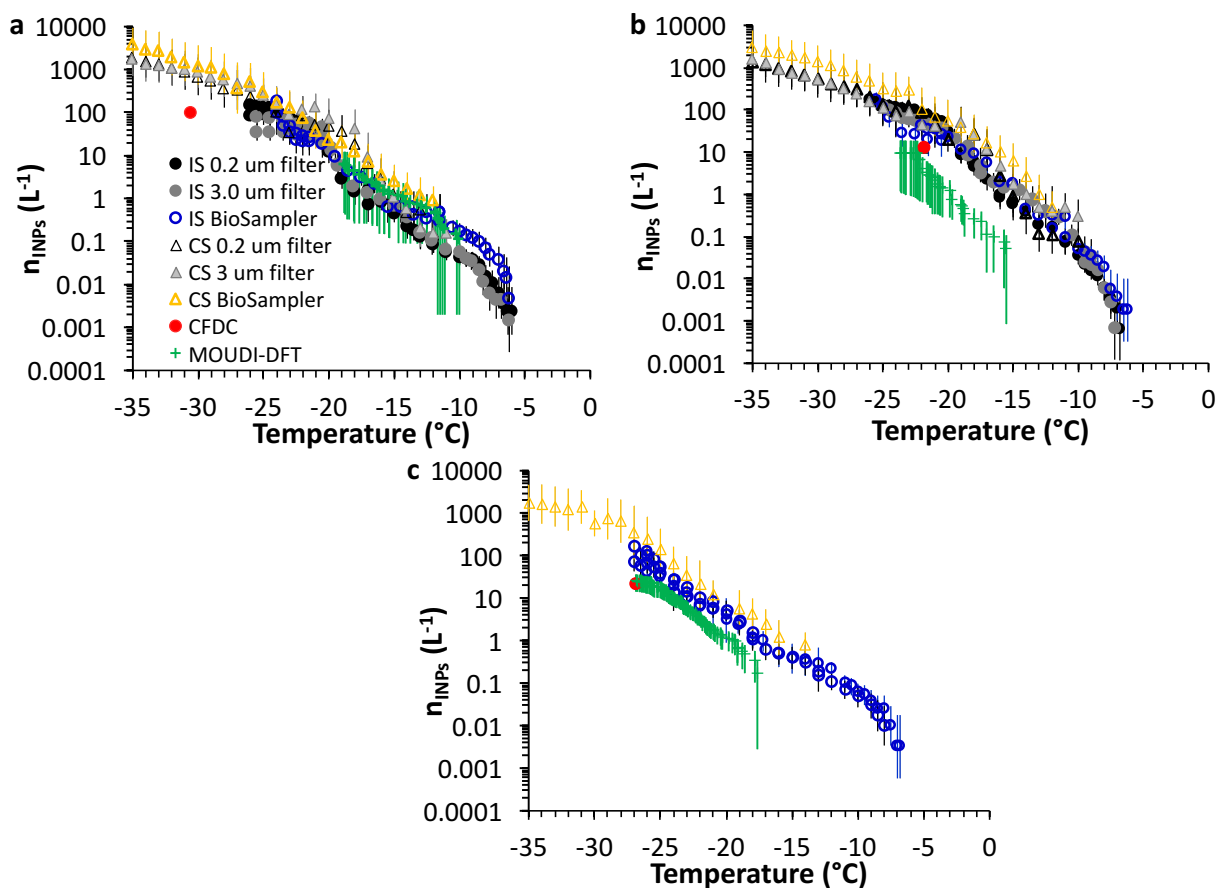
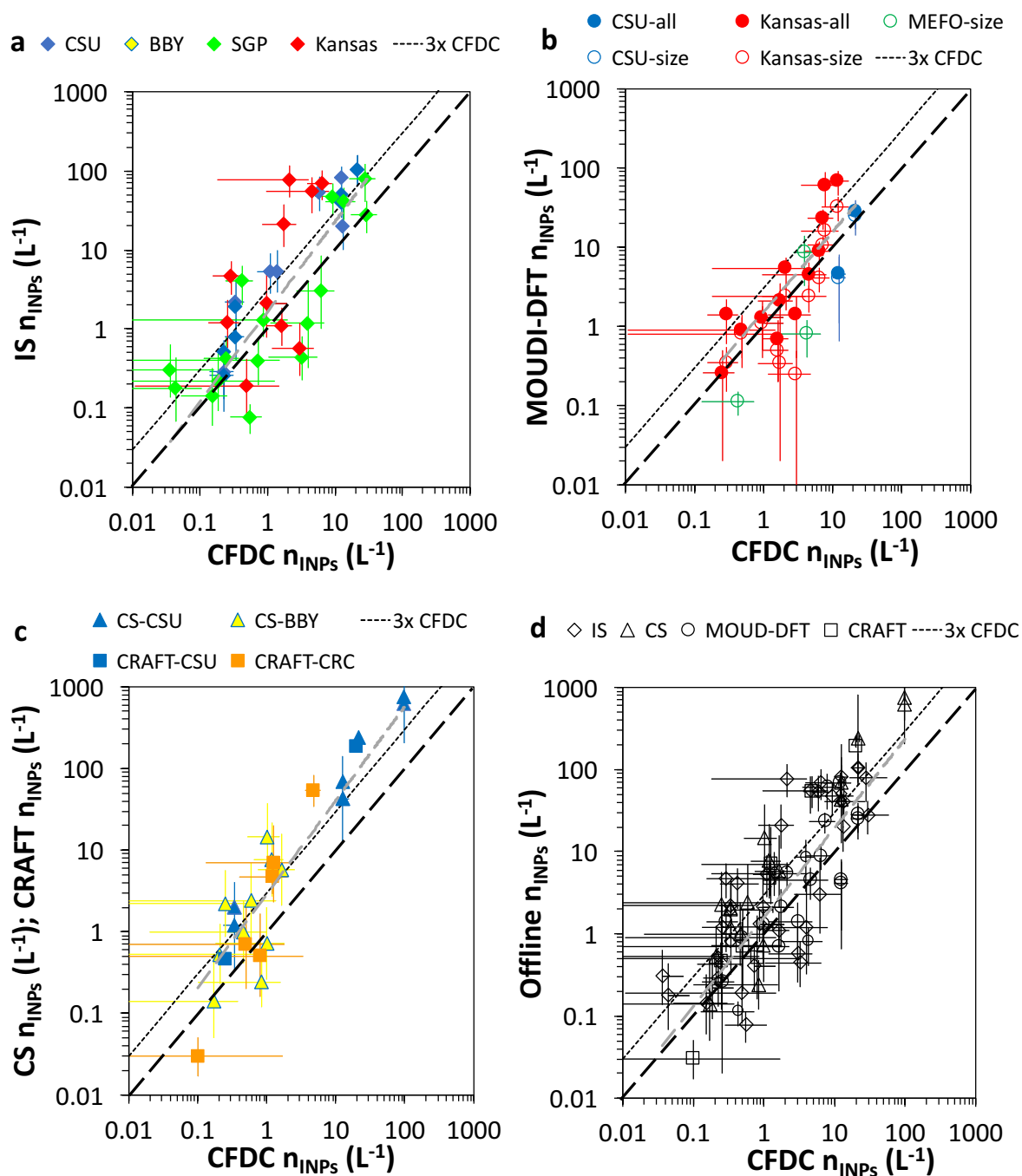


**Figure 1.** Temperature spectra of INP number concentrations ( $n_{INP}$ ) from IS and CS measurements and a CFDC measuring at a single temperature over a 4-hour sampling period. Ambient aerosols were sampled outside of the Colorado State University Atmospheric Chemistry building on a) September 12, 2013; and b) September 6, 2013. Temperature spectra were separately measured for simultaneously collected filter samples with different pore sizes and liquid samples from a BioSampler. Uncertainty values (95% confidence intervals) are shown.

1235



1240 **Figure 2.** Three additional experimental comparison days, as in Fig. 1, but for cases where all four methods were  
 1245 operational for consistent sampling periods. These dates were November 12 through 14 in panels a), b), c),  
 1250 respectively. The legend is shown in panel a). The additional data in green are from the MOUDI-DFT method (all  
 sizes included), including median (cross), upper and lower bounds.



1255 **Figure 3.** Scatter plot of INP number concentrations obtained with different immersion freezing methods plotted  
 against CFDC online measurement results obtained at 105% RH and temperatures ranging from approximately -15  
 to -31°C: (a) IS, (b) MOUDI-DFT (medians of data such as shown in Fig. 1), (c) CS and CRAFT, (d) all data  
 combined from offline immersion freezing tests. The MOUDI-DFT data in (b) include data for all particles sizes  
 assessed (“all”) and for the particle size range of 0.3-3.2  $\mu\text{m}$  (“size”) best aligned with the effective CFDC sampling  
 size range. Error bars represent 95% confidence intervals, as defined for each method. Light dashed gray lines are  
 1260 simple linear relations intended only to guide the eye.

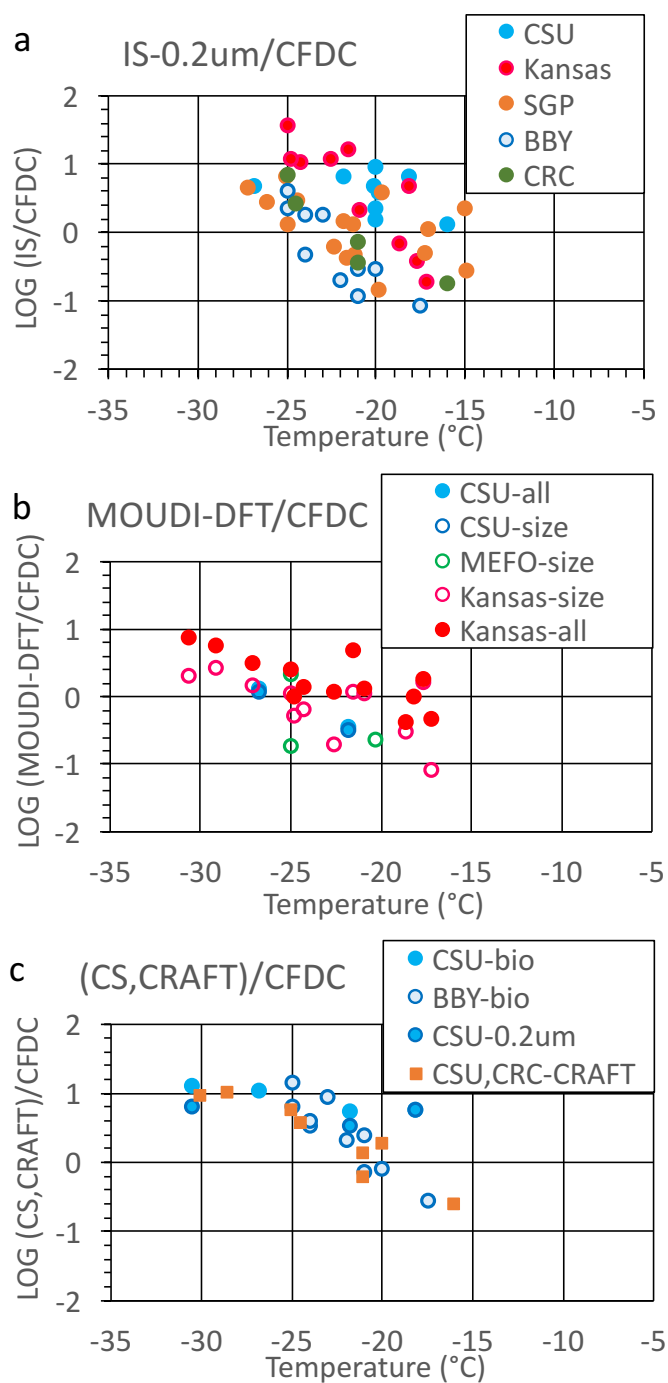
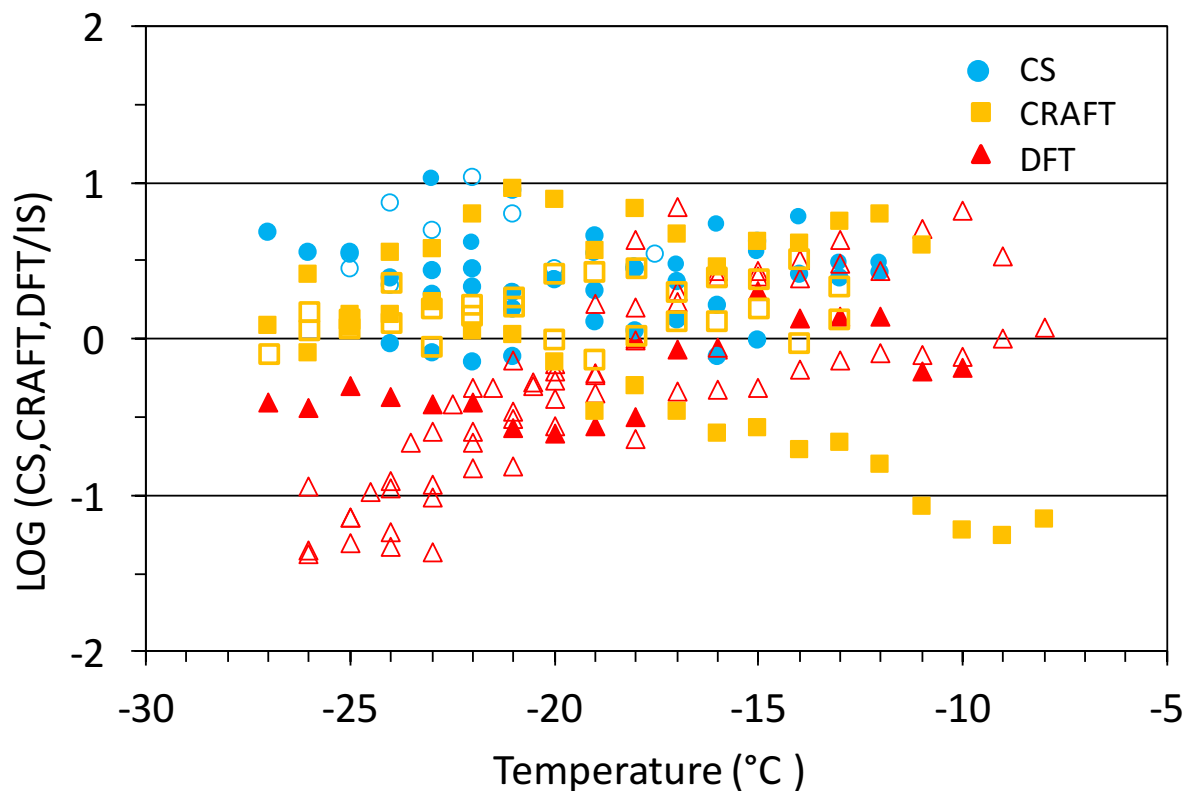


**Figure 4.** Logarithm of the ratio of INP number concentrations measured by various immersion freezing methods versus the CFDC at different sites, denoted as in previous figures. IS 0.2  $\mu\text{m}$  filter samples are shown in a) from five sites. MOUDI-DFT data are compared from three sites in b), where “size” and “all” refer to whether INP number concentrations are from MOUDI size ranges overlapping with sizes permitted into the CFDC or from all sizes. CS and CRAFT ratios are shown in c), where all blue points are for the CS, and “bio” refers to BioSampler collections.

1270



1275

**Figure 5.** Immersion freezing methods comparison, shown as the base-ten logarithm of the ratio of the CS, CRAFT and MOUDI-DFT method INP concentrations for perfect or imperfect overlap of co-sampling periods with the IS INP number concentrations. Samples collected outside the CSU Atmospheric Chemistry facility are shown as filled symbols, while samples collected at other sites on different days (CS: Bodega Bay; CRAFT: Canyonlands Research Center; DFT: Colby, KS) are shown as open symbols.

1280

1285

Supplement of

**Comparative measurements of ambient atmospheric concentrations of ice nucleating particles using multiple immersion freezing methods and a continuous flow diffusion chamber**

1290

P. J. DeMott et al.

Correspondence to: Paul J. DeMott (Paul.Demott@colostate.edu)

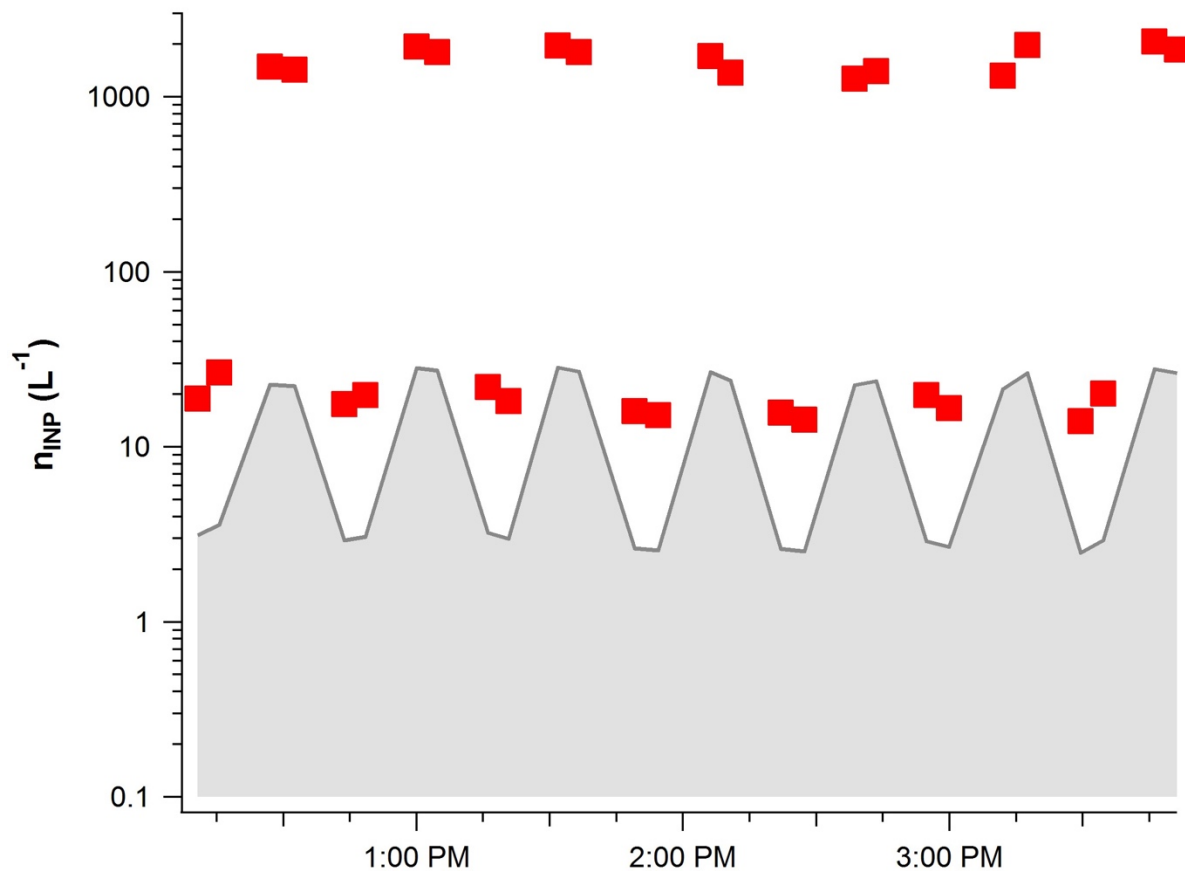


**Figure S1.** Aerosol Concentrator calibration check at  $-30^{\circ}\text{C}$  at CSU on May 19, 2016. This is a typical experimental sampling period at one temperature. In this figure, the lower data points are INP number concentrations without using the aerosol concentrator. Alternating periods of high INP number concentrations are during use of the aerosol concentrator. Inspection of the ratio between the INP number concentrations per volume of air during periods on versus off the concentrator reveal the CF factor, which is  $\sim 90$  in this case. The shaded lower region is the limit of significance for INP concentrations, as described in Section 2.1 of the manuscript.

1295

1300

1305

**Table S1.** Data for Figures 3 and 4. INP concentrations and confidence limits (CL+; CL-) are in units L<sup>-1</sup>, and Temp is in °C. Concentrator (Y: On; N: Off; B: both on and off for integrated period). IS pore-size and CS pore-size or BioSampler (Bio) use are indicated.

Date	Site	Temp	CFDC	CFDC_CL-	CFDC_CL+	Concentrator	IS_0.2um	IS_CL-	IS_CL+	IS_3um	IS_CL-	IS_CL+
29-Sep-10	NoCO Ag	-19.9	1.40	0.30	0.20	N	5.40	2.50	4.50			
4-Oct-10	NoCO Ag	-20.0	13.20	0.20	0.20	N	20.00	10.00	18.80			
8-Oct-10	NoCO Ag	-20.1	1.10	0.40	0.40	N	5.30	2.50	3.75			
3-Nov-10	NoCO Ag	-20.0	5.90	1.00	1.00	N	53.00	22.00	31.00			
6-Sep-13	CSU ATChem	-18.2	0.34	0.11	0.11	Y	2.20	1.20	2.00	1.90	0.92	1.80
12-Sep-13	CSU ATChem	-16.0	0.23	0.09	0.09	Y	0.29	0.16	0.32	0.52	0.25	0.41
12-Nov-13	CSU ATChem	-30.5	98.00	13.00	12.00	N						
13-Nov-13	CSU ATChem	-21.8	12.50	2.50	3.00	N	81.00	26.00	32.00	42.00	17.70	22.00
14-Nov-13	CSU ATChem	-26.8	21.50	4.50	4.50	N	105.00	41.00	53.00			
18-May-16	CSU ATChem	-20.0	0.25	0.02	0.02	Y	0.55	0.27	0.46			
19-May-16	CSU ATChem	-30.0	20.00	0.20	0.20	Y						
11-May-16	CRC (all STP)	-21.0	0.82	0.81	2.56	N	0.29	0.12	0.18			
11-May-16	CRC (all STP)	-25.0	1.25	1.4	1.24	N	8.50	3.20	3.77			
12-May-16	CRC (all STP)	-16.0	0.12	1.80	0.11	N	0.02	0.01	0.02			
12-May-16	CRC (all STP)	-21.0	0.51	1.40	0.51	N	0.38	0.19	0.31			
12-May-16	CRC (all STP)	-24.5	1.30	0.88	0.88	N	3.40	1.50	3.00			
12-May-16	CRC (all STP)	-28.5	5.20	1.30	1.30	N						
26-Jan-15	BBY	-17.5	0.84	0.74	0.74	B	0.07	0.04	0.12			
26-Jan-15	BBY	-21.0	0.99	0.81	0.81	Y	0.12	0.07	0.14			
26-Jan-15	BBY	-23.0	0.25	0.24	0.50	Y	0.45	0.20	0.27			
26-Jan-15	BBY	-24.0	1.64	0.90	0.90	Y	0.78	0.33	0.40			
26-Jan-15	BBY	-25.0	1.02	0.50	0.50	Y	4.20	2.17	3.70			
2-Feb-15	BBY	-20.0	0.17	0.16	0.21	Y	0.05	0.03	0.02			
2-Feb-15	BBY	-21.0	0.21	0.20	0.65	N	0.06	0.02	0.03			
2-Feb-15	BBY	-22.0	0.46	0.44	0.55	Y	0.09	0.04	0.05			
2-Feb-15	BBY	-24.0	0.59	0.58	0.76	B	1.10	0.46	0.65			
2-Feb-15	BBY	-25.0	1.19	0.54	0.54	B	2.74	1.07	1.29			
30-Apr-14	SGP	-21.2	0.84	0.82	0.82	B	0.40	0.21	0.35			
30-Apr-14	SGP	-27.2	10.59	4.75	4.75	B	47.64	19.80	21.60			
4-May-14	SGP	-21.6	2.75	2.40	2.40	B	1.19	0.87	2.92			
4-May-14	SGP	-24.9	21.05	8.96	8.96	B	27.89	11.61	13.66			
4-May-14	SGP	-15.0	0.28	0.13	0.13	Y	0.08	0.03	0.03			
5-May-14	SGP	-19.9	2.98	2.11	2.11	B	0.44	0.22	0.36			
5-May-14	SGP	-22.4	4.85	2.99	2.99	B	3.03	2.02	5.43			
5-May-14	SGP	-24.4	13.55	6.36	6.36	N	40.74	16.75	20.16			
5-May-14	SGP	-26.1	27.80	11.65	11.65	B	79.55	39.21	42.74			
5-Jun-14	SGP	-19.7	0.08	0.07	0.27	B	0.30	0.17	0.33			
7-Jun-14	SGP	-17.1	0.19	0.18	1.12	B	0.22	0.13	0.27			
7-Jun-14	SGP	-21.3	0.32	0.17	0.17	Y	0.43	0.21	0.35			
7-Jun-14	SGP	-25.1	0.61	0.27	0.27	Y	4.05	2.03	2.23			
8-Jun-14	SGP	-15.0	0.08	0.07	0.11	Y	0.18	0.11	0.26			
8-Jun-14	SGP	-21.8	0.89	0.88	1.15	Y	1.30	0.50	0.65			
30-Apr-14	SGP	-17.2	0.29	0.19	0.19	Y	0.14	0.08	0.18			
14-Oct-14	Kansas-harvest	-18.7	1.63	0.66	0.66	Y	1.10	0.49	0.75			
14-Oct-14	Kansas-harvest	-24.3	6.43	2.58	2.58	Y	69.00	26.40	31.90			
14-Oct-14	Kansas-harvest	-29.2	12.06	5.12	5.12	Y						
15-Oct-14	Kansas-harvest	-17.2	3.00	1.84	1.84	Y	0.57	0.31	0.63			
15-Oct-14	Kansas-harvest	-22.6	1.74	0.91	0.91	Y	21.00	10.10	16.50			
15-Oct-14	Kansas-harvest	-27.1	7.29	2.93	2.93	Y						
10/15/2014-10/16/2014	Kansas	-18.2	0.26	0.12	0.12	Y	1.20	0.62	1.13			
10/15/2014-10/16/2014	Kansas	-21.6	0.29	0.14	0.14	Y	4.70	1.99	2.49			
10/15/2014-10/16/2014	Kansas	-25.0	2.12	1.94	1.94	Y	77.03	30.88	39.60			
14-Oct-14	Kansas	-17.7	0.49	0.48	1.00	Y	0.19	0.11	0.23			
14-Oct-14	Kansas	-20.9	0.97	0.97	0.98	Y	2.10	1.32	3.14			
14-Oct-14	Kansas	-24.8	4.54	3.59	3.59	Y	55.00	25.90	27.70			
14-Oct-14	Kansas	-30.7	7.84	4.35	4.35	Y						
17-Aug-11	MEFO	-25.0	3.92	1.22	1.22	Y						
17-Aug-11	MEFO	-25.0	4.26	2.48	2.48	Y						
18-Aug-11	MEFO	-20.3	0.43	0.30	0.30	Y						

1310 Table S1. (continued)

Date	Site	Temp	IS-Biosamp	IS_CL-	IS_CL+CS_0.2um	CS_CL-	CS_CL+CS_3um	CS_CL-	CS_CL+		
29-Sep-10	NoCO Ag	-19.9									
4-Oct-10	NoCO Ag	-20.0									
8-Oct-10	NoCO Ag	-20.1									
3-Nov-10	NoCO Ag	-20.0									
6-Sep-13	CSU ATChem	-18.2	0.80	0.35	0.55	2.02	1.25	3.26	1.20	0.88	2.86
12-Sep-13	CSU ATChem	-16.0	0.26	0.17	0.46						
12-Nov-13	CSU ATChem	-30.5				624.06	443.30	1250.50	752.79	548.80	1348.50
13-Nov-13	CSU ATChem	-21.8	40.00	19.00	21.00	42.90	27.30	75.30	42.40	29.70	98.90
14-Nov-13	CSU ATChem	-26.8	105.00	40.50	52.30						
18-May-16	CSU ATChem	-20.0									
19-May-16	CSU ATChem	-30.0									
11-May-16	CRC (all STP)	-21.0									
11-May-16	CRC (all STP)	-25.0									
12-May-16	CRC (all STP)	-16.0									
12-May-16	CRC (all STP)	-21.0									
12-May-16	CRC (all STP)	-24.5									
12-May-16	CRC (all STP)	-28.5									
26-Jan-15	BBY	-17.5									
26-Jan-15	BBY	-21.0									
26-Jan-15	BBY	-23.0									
26-Jan-15	BBY	-24.0									
26-Jan-15	BBY	-25.0									
2-Feb-15	BBY	-20.0									
2-Feb-15	BBY	-21.0									
2-Feb-15	BBY	-22.0									
2-Feb-15	BBY	-24.0									
2-Feb-15	BBY	-25.0									
30-Apr-14	SGP	-21.2									
30-Apr-14	SGP	-27.2									
4-May-14	SGP	-21.6									
4-May-14	SGP	-24.9									
4-May-14	SGP	-15.0									
5-May-14	SGP	-19.9									
5-May-14	SGP	-22.4									
5-May-14	SGP	-24.4									
5-May-14	SGP	-26.1									
5-Jun-14	SGP	-19.7									
7-Jun-14	SGP	-17.1									
7-Jun-14	SGP	-21.3									
7-Jun-14	SGP	-25.1									
8-Jun-14	SGP	-15.0									
8-Jun-14	SGP	-21.8									
30-Apr-14	SGP	-17.2									
14-Oct-14	Kansas-harvest	-18.7									
14-Oct-14	Kansas-harvest	-24.3									
14-Oct-14	Kansas-harvest	-29.2									
15-Oct-14	Kansas-harvest	-17.2									
15-Oct-14	Kansas-harvest	-22.6									
15-Oct-14	Kansas-harvest	-27.1									
10/15/2014-10/16/2014	Kansas	-18.2									
10/15/2014-10/16/2014	Kansas	-21.6									
10/15/2014-10/16/2014	Kansas	-25.0									
14-Oct-14	Kansas	-17.7									
14-Oct-14	Kansas	-20.9									
14-Oct-14	Kansas	-24.8									
14-Oct-14	Kansas	-30.7									
17-Aug-11	MEFO	-25.0									
17-Aug-11	MEFO	-25.0									
18-Aug-11	MEFO	-20.3									

**Table S1. (continued)**

Date	Site	Temp	CS_Biosamp	CS_CL-	CS_CL+ DFT_all	DFT_CLDFT_size	DFT_CL	CRAFT	CRAFT_CL-	CRAFT_CL+
29-Sep-10	NoCO Ag	-19.9								
4-Oct-10	NoCO Ag	-20.0								
8-Oct-10	NoCO Ag	-20.1								
3-Nov-10	NoCO Ag	-20.0								
6-Sep-13	CSU ATChem	-18.2	1.98	1.12	2.60					
12-Sep-13	CSU ATChem	-16.0								
12-Nov-13	CSU ATChem	-30.5	1281.00	884.00	2389.00					
13-Nov-13	CSU ATChem	-21.8	69.60	45.80	134.30	4.59	3.49	4.12	3.47	
14-Nov-13	CSU ATChem	-26.8	238.00	168.70	579.00	28.10	11.10	25.20	11.10	
18-May-16	CSU ATChem	-20.0						0.46	0.34	1.17
19-May-16	CSU ATChem	-30.0						188.2	59.4	68
11-May-16	CRC (all STP)	-21.0						0.5	0.34	1.17
11-May-16	CRC (all STP)	-25.0						7	4.7	13
12-May-16	CRC (all STP)	-16.0						0.03	0.013	0.021
12-May-16	CRC (all STP)	-21.0						0.7	0.5	1.3
12-May-16	CRC (all STP)	-24.5						4.7	1.8	2.7
12-May-16	CRC (all STP)	-28.5						54	20	29
26-Jan-15	BBY	-17.5	0.24	0.12	0.24					
26-Jan-15	BBY	-21.0	0.72	0.46	1.28					
26-Jan-15	BBY	-23.0	2.22	1.35	3.45					
26-Jan-15	BBY	-24.0	5.76	3.66	10.06					
26-Jan-15	BBY	-25.0	14.56	8.92	23.02					
2-Feb-15	BBY	-20.0	0.14	0.09	0.36					
2-Feb-15	BBY	-21.0	0.53	0.3	0.72					
2-Feb-15	BBY	-22.0	0.99	0.58	1.42					
2-Feb-15	BBY	-24.0	2.39	1.57	4.57					
2-Feb-15	BBY	-25.0	7.66	4.96	14.04					
30-Apr-14	SGP	-21.2								
30-Apr-14	SGP	-27.2								
4-May-14	SGP	-21.6								
4-May-14	SGP	-24.9								
4-May-14	SGP	-15.0								
5-May-14	SGP	-19.9								
5-May-14	SGP	-22.4								
5-May-14	SGP	-24.4								
5-May-14	SGP	-26.1								
5-Jun-14	SGP	-19.7								
7-Jun-14	SGP	-17.1								
7-Jun-14	SGP	-21.3								
7-Jun-14	SGP	-25.1								
8-Jun-14	SGP	-15.0								
8-Jun-14	SGP	-21.8								
30-Apr-14	SGP	-17.2								
14-Oct-14	Kansas-harvest	-18.7				0.70	0.50	0.50	0.30	
14-Oct-14	Kansas-harvest	-24.3				8.90	2.90	4.10	1.40	
14-Oct-14	Kansas-harvest	-29.2				68.50	23.50	32.30	11.00	
15-Oct-14	Kansas-harvest	-17.2				1.40	1.00	0.25	0.24	
15-Oct-14	Kansas-harvest	-22.6				2.10	1.40	0.34	0.32	
15-Oct-14	Kansas-harvest	-27.1				23.30	6.60	10.70	2.90	
10/15/2014-10/16/2014	Kansas	-18.2				0.26	0.24			
10/15/2014-10/16/2014	Kansas	-21.6				1.40	0.80	0.35	0.20	
10/15/2014-10/16/2014	Kansas	-25.0				5.40	2.00	2.40	0.80	
14-Oct-14	Kansas	-17.7				0.90	0.50	0.80	0.50	
14-Oct-14	Kansas	-20.9				1.30	0.80	1.10	0.70	
14-Oct-14	Kansas	-24.8				4.50	1.90	2.40	0.90	
14-Oct-14	Kansas	-30.7				60.80	28.10	16.00	4.50	
17-Aug-11	MEFO	-25.0					8.60	5.35		
17-Aug-11	MEFO	-25.0					0.8	0.40		
18-Aug-11	MEFO	-20.3					0.1	0.04		

**Table S2.** Data for Figure 5. Instrument name column data and positive (+) and negative (-) confidence intervals are INP concentrations in L<sup>-1</sup>, and T is in °C. “Bio” indicates use of the BioSampler, while all other samples used 0.2 μm pore size filters for collections.

Location	Date	T	CS	CS+	CS-	IS	IS+	IS-	LOG(CS/IS)
BBY	1/26/15	-17.5	0.240	0.240	0.120	0.070	0.118	0.044	0.535
		-21.0	0.720	1.280	0.460	0.116	0.141	0.068	0.794
		-23.0	2.220	3.450	1.350	0.450	0.270	0.197	0.693
		-24.0	5.760	10.060	3.660	0.780	0.403	0.329	0.868
		-25.0	14.560	23.020	8.920	4.200	3.702	2.171	0.540
BBY	2/2/15	-20.0	0.140	0.360	0.090	0.050	0.021	0.031	0.448
		-21.0	0.530	0.720	0.300	0.060	0.034	0.025	0.945
		-22.0	0.990	1.420	0.580	0.093	0.045	0.035	1.028
		-24.0	2.390	4.570	1.570	1.098	0.654	0.457	0.338
		-25.0	7.660	14.040	4.960	2.736	1.290	1.074	0.447
Kansas	14-Oct-14	T MOUDI-DFT	DFT+	DFT-	IS	IS+	IS-	LOG(DFT/IS)	
		-15.0	0.210	0.200	0.200	0.078	0.191	0.057	0.428
		-16.0	0.210	0.200	0.200	0.078	0.191	0.057	0.428
		-17.0	0.550	0.460	0.460	0.078	0.191	0.057	0.846
		-18.0	0.900	0.500	0.500	0.210	0.257	0.123	0.631
		-19.0	1.040	0.500	0.500	0.624	0.418	0.284	0.222
		-20.0	1.110	0.640	0.640	1.613	0.823	0.690	-0.162
		-20.5	1.190	0.700	0.700	2.237	1.153	1.019	-0.274
		-20.0	1.100	0.640	0.640	1.772	3.220	1.179	-0.207
		-20.5	1.190	0.700	0.700	2.404	3.527	1.486	-0.305
		-21.0	1.750	0.890	0.890	2.404	3.527	1.486	-0.138
		-21.5	1.840	0.920	0.920	3.738	4.103	2.062	-0.308
		-22.0	2.260	1.100	1.100	4.608	4.533	2.430	-0.309
		-22.5	2.690	1.230	1.230	7.012	5.417	3.313	-0.416
		-23.0	3.300	1.380	1.380	13.069	7.461	5.358	-0.598
-23.5	4.450	1.930	1.930	20.369	9.943	7.839	-0.661		
-24.0	4.590	1.940	1.940	36.865	16.591	14.488	-0.905		
-24.5	6.560	2.850	2.850	61.823	31.151	29.048	-0.974		
Kansas	10/1514-10/16/14	T MOUDI-DFT	DFT+	DFT-	IS	IS+	IS-	LOG(DFT/IS)	
		-8.0	0.070	0.067	0.067	0.059	0.056	0.031	0.074
		-9.0	0.100	0.100	0.100	0.104	0.074	0.049	0.000
		-10.0	0.100	0.100	0.100	0.132	0.084	0.059	-0.114
		-11.0	0.150	0.140	0.140	0.186	0.105	0.080	-0.103
		-12.0	0.150	0.150	0.150	0.186	0.105	0.080	-0.094
		-13.0	0.170	0.150	0.150	0.235	0.125	0.099	-0.141
		-14.0	0.170	0.150	0.150	0.266	0.138	0.113	-0.195
		-15.0	0.170	0.150	0.150	0.353	0.179	0.154	-0.317
		-16.0	0.200	0.180	0.180	0.422	0.217	0.192	-0.324
		-17.0	0.250	0.220	0.220	0.539	0.293	0.268	-0.334
		-18.0	0.270	0.250	0.250	1.170	1.126	0.622	-0.637
		-19.0	0.620	0.420	0.420	1.376	1.207	0.704	-0.346
		-20.0	0.760	0.460	0.460	1.829	1.381	0.877	-0.381
		-21.0	1.160	0.660	0.660	3.728	2.096	1.592	-0.507
-22.0	1.570	0.800	0.800	10.640	5.867	5.343	-0.831		
-23.0	2.260	1.100	1.100	23.274	19.293	11.364	-1.013		
-24.0	3.140	1.200	1.200	53.948	29.684	21.755	-1.235		
-25.0	5.610	2.100	2.100	77.026	39.603	30.877	-1.138		
-26.0	7.570	2.600	2.600	179.101	87.033	78.307	-1.376		
Kansas harvest soy	14-Oct-14	T MOUDI-DFT	DFT+	DFT-	IS	IS+	IS-	LOG(DFT/IS)	
		-16.0	0.230	0.230	0.230	0.265	0.117	0.103	-0.061
		-17.0	0.520	0.300	0.300	0.301	0.135	0.121	0.237
		-18.0	0.720	0.400	0.400	0.732	0.659	0.370	-0.007
		-19.0	0.720	0.550	0.550	1.196	0.822	0.533	-0.220
		-20.0	0.820	0.630	0.630	2.960	1.411	1.122	-0.558
		-21.0	1.040	0.670	0.670	6.797	9.973	4.202	-0.815
		-22.0	2.180	1.010	1.010	8.648	10.799	5.028	-0.598
		-23.0	4.140	1.560	1.560	35.281	20.186	14.416	-0.931
		-24.0	8.430	2.880	2.880	76.000	34.812	28.865	-0.955
-25.0	12.850	3.820	3.820	180.000	223.096	104.167	-1.146		
-26.0	25.000	7.150	7.150	220.000	239.811	120.883	-0.944		

1320 **Table S2.** (continued)

Kansas harvest sorghum	15-Oct-14	T	MOUDI-DFT	DFT+	DFT-	IS	IS+	IS-	LOG(DFT/IS)		
				-9.0	0.350	0.340	0.340	0.104	0.059	0.042	0.528
				-10.0	1.140	0.854	0.854	0.174	0.083	0.066	0.816
				-11.0	1.140	0.854	0.854	0.228	0.103	0.086	0.700
				-12.0	1.140	0.854	0.854	0.415	0.192	0.175	0.439
				-13.0	1.260	0.908	0.908	0.415	0.192	0.175	0.482
				-14.0	1.260	0.908	0.908	0.519	0.259	0.242	0.385
				-13.0	1.260	0.908	0.908	0.295	0.536	0.196	0.631
				-14.0	1.260	0.908	0.908	0.400	0.587	0.247	0.498
				-15.0	1.260	0.908	0.908	0.509	0.635	0.296	0.394
				-16.0	1.260	0.908	0.908	0.509	0.635	0.296	0.394
				-17.0	1.260	0.908	0.908	0.622	0.683	0.343	0.307
				-18.0	1.580	1.136	1.136	0.989	0.822	0.482	0.203
				-19.0	1.580	1.136	1.136	2.698	1.392	1.053	-0.232
				-20.0	1.910	1.358	1.358	3.483	1.660	1.320	-0.261
				-21.0	2.020	1.402	1.402	5.900	10.714	3.923	-0.466
				-22.0	2.160	1.447	1.447	10.000	12.707	5.917	-0.666
				-23.0	2.490	1.503	1.503	57.000	29.303	22.305	-1.360
				-24.0	4.030	1.689	1.689	86.000	211.495	62.475	-1.329
		-25.0	8.790	2.870	2.870	180.000	259.082	110.061	-1.311		
		-26.0	14.550	4.683	4.683	330.000	323.840	174.819	-1.356		
CRC	11-May-16	T	CRAFT	CRAFT+	CRAFT-	IS	IS+	IS-	LOG(CRAFT/IS)		
				-13.0	0.005	0.012	0.003	0.002	0.009	0.002	0.333
				-14.0	0.007	0.013	0.005	0.002	0.009	0.002	0.514
				-15.0	0.015	0.016	0.008	0.009	0.013	0.006	0.197
				-16.0	0.023	0.019	0.011	0.009	0.013	0.006	0.389
				-17.0	0.041	0.025	0.016	0.020	0.018	0.010	0.297
				-18.0	0.099	0.041	0.033	0.035	0.023	0.016	0.454
				-19.0	0.188	0.068	0.059	0.070	0.037	0.030	0.429
				-20.0	0.432	0.192	0.184	0.167	0.139	0.081	0.413
				-21.0	0.463	1.175	0.337	0.291	0.181	0.124	0.202
				-22.0	1.195	1.529	0.691	0.858	1.072	0.499	0.144
				-23.0	2.822	2.111	1.273	3.195	1.547	0.974	-0.054
		-24.0	6.213	3.087	2.249	4.954	2.484	1.911	0.098		
		-25.0	11.118	4.422	3.584	8.454	3.769	3.197	0.119		
		-26.0	20.121	7.230	6.392	13.677	6.481	5.872	0.168		
CRC	12-May-16	T	CRAFT	CRAFT+	CRAFT-	IS	IS+	IS-	LOG(CRAFT/IS)		
				-13.0	0.002	0.010	0.002	0.002	0.007	0.001	0.126
				-14.0	0.007	0.013	0.005	0.007	0.011	0.005	-0.022
				-15.0	0.023	0.019	0.011	0.009	0.012	0.006	0.387
				-16.0	0.028	0.021	0.013	0.022	0.016	0.010	0.113
				-17.0	0.041	0.025	0.016	0.032	0.020	0.014	0.110
				-18.0	0.066	0.032	0.024	0.063	0.033	0.027	0.019
				-19.0	0.094	0.040	0.031	0.128	0.070	0.064	-0.135
				-20.0	0.188	0.068	0.059	0.189	0.230	0.110	-0.001
				-21.0	0.702	1.304	0.466	0.380	0.308	0.188	0.267
				-22.0	1.451	1.633	0.795	0.888	0.499	0.379	0.213
				-23.0	2.254	1.925	1.087	1.422	0.738	0.615	0.200
		-24.0	3.738	2.392	1.554	1.628	0.853	0.725	0.361		
		-25.0	6.216	3.089	2.251	5.309	5.128	2.818	0.069		
		-26.0	10.524	4.258	3.420	9.371	6.669	4.358	0.050		
		-27.0	20.132	7.234	6.396	25.182	14.644	11.668	-0.097		

1325

Table S2. (continued)

1330

CSU	18-May-16	T	CRAFT	CRAFT+	CRAFT-	IS	IS+	IS-	LOG(CRAFT/IS)		
		-8.0	0.002	0.010	0.002	0.025	0.022	0.013	-1.160		
		-9.0	0.007	0.013	0.005	0.098	0.051	0.042	-1.261		
		-10.0	0.012	0.015	0.007	0.156	0.080	0.071	-1.229		
		-11.0	0.017	0.017	0.009	0.156	0.080	0.071	-1.073		
		-12.0	0.034	0.023	0.015	0.168	0.298	0.112	-0.804		
		-13.0	0.047	0.027	0.018	0.168	0.298	0.112	-0.663		
		-14.0	0.058	0.030	0.021	0.229	0.329	0.142	-0.708		
		-15.0	0.079	0.036	0.027	0.229	0.329	0.142	-0.574		
		-16.0	0.118	0.046	0.038	0.361	0.387	0.201	-0.601		
		-17.0	0.156	0.057	0.049	0.352	0.399	0.201	-0.466		
		-18.0	0.278	0.103	0.095	0.428	0.431	0.233	-0.301		
		-19.0	0.229	1.027	0.189	0.509	0.464	0.266	-0.461		
		-20.0	0.463	1.175	0.337	0.509	0.464	0.266	-0.155		
		-21.0	0.702	1.304	0.466	0.509	0.483	0.272	0.025		
		-22.0	1.196	1.530	0.691	0.812	0.604	0.393	0.054		
		-23.0	3.120	2.205	1.367	1.379	0.831	0.620	0.241		
		-24.0	6.620	3.199	2.360	3.575	2.168	1.916	0.154		
		-25.0	11.124	4.425	3.586	7.224	8.657	4.245	0.074		
		-26.0	16.595	6.047	5.209	15.970	13.469	8.353	-0.097		
		-27.0	43.230	19.237	18.398	27.586	19.757	14.032	0.081		
		CSU	19-May-16	T	CRAFT	CRAFT+	CRAFT-	IS	IS+	IS-	LOG(CRAFT/IS)
				-11.0	0.020	0.018	0.010	0.005	0.012	0.004	0.598
				-12.0	0.031	0.022	0.014	0.005	0.012	0.004	0.796
				-13.0	0.058	0.030	0.021	0.010	0.015	0.007	0.745
				-14.0	0.124	0.048	0.040	0.031	0.023	0.015	0.604
				-15.0	0.188	0.068	0.059	0.045	0.029	0.020	0.623
-16.0	0.229			1.027	0.189	0.080	0.042	0.034	0.459		
-17.0	0.463			1.175	0.337	0.099	0.052	0.043	0.669		
-18.0	0.946			1.421	0.582	0.139	0.073	0.064	0.833		
-19.0	0.946			1.421	0.582	0.256	0.335	0.154	0.567		
-20.0	1.980			1.830	0.992	0.256	0.335	0.154	0.888		
-21.0	2.824			2.112	1.274	0.312	0.376	0.183	0.956		
-22.0	3.425			2.298	1.460	0.551	0.477	0.284	0.794		
-23.0	6.216			3.089	2.251	1.648	0.926	0.733	0.577		
-24.0	8.895	3.813	2.975	2.474	1.464	1.234	0.556				
-25.0	11.956	15.297	6.913	8.335	7.987	4.439	0.157				
-26.0	25.355	20.192	11.808	9.895	9.339	5.303	0.409				
CSU	6-Sep-13	T	CS	CS+	CS-	IS	IS+	IS-	LOG(CS/IS)		
		-15	0.584	0.584	0.292	0.567	0.331	0.245	-0.013		
		-16	0.806	1.122	0.469	0.621	0.351	0.266	-0.113		
		-17	1.163	1.876	0.718	1.545	1.732	0.874	0.123		
		-18	2.017	3.257	1.246	2.236	2.014	1.156	0.045		
		-19	2.697	4.820	1.729	3.411	2.462	1.604	0.102		
		-21	11.097	17.508	6.792	8.567	4.478	3.620	-0.112		
		-22	21.839	44.909	14.693	15.670	17.416	8.835	-0.144		
		-23	33.488	76.010	23.246	26.778	21.857	13.276	-0.097		
CSU	12-Nov-13	T	CS-Bio	CS+	CS-	IS-Bio	IS+	IS-	LOG(CS/IS)		
		-12.0	0.954	0.954	0.477	0.364	0.163	0.146	0.418		
		-13.0	1.258	1.833	0.746	0.514	0.754	0.318	0.389		
		-14.0	1.693	2.318	0.978	0.653	0.816	0.380	0.413		
		-15.0	2.712	3.340	1.497	0.653	0.816	0.380	0.618		
		-16.0	3.781	7.196	2.479	2.299	1.405	0.969	0.216		
		-17.0	7.550	11.301	4.526	3.277	1.726	1.290	0.362		
		-18.0	12.922	19.174	7.720	4.631	2.187	1.751	0.446		
		-19.0	20.698	29.290	12.128	4.631	2.187	1.751	0.650		
		-20.0	24.259	33.646	14.096	10.126	4.632	4.196	0.379		
		-21.0	39.027	64.816	24.360	19.965	21.915	11.014	0.291		
		-22.0	75.870	115.796	45.837	27.063	24.670	13.769	0.448		
-23.0	138.679	189.600	80.095	51.655	33.204	22.303	0.429				
-24.0	181.408	208.552	97.018	195.255	86.523	75.622	-0.032				

**Table S2. (continued)**

CSU	12-Nov-13	T	MOUDI-DFT	DFT+	DFT-	IS-Bio	IS+	IS-	LOG(DFT/IS)
		-10.0	0.118	0.116	0.116	0.179	0.085	0.068	-0.180
		-11.0	0.200	0.198	0.198	0.320	0.142	0.124	-0.203
		-12.0	0.508	0.423	0.423	0.364	0.163	0.146	0.145
		-13.0	0.710	0.622	0.622	0.514	0.754	0.318	0.141
		-14.0	0.891	0.801	0.801	0.653	0.816	0.380	0.134
		-15.0	1.314	1.193	1.193	0.653	0.816	0.380	0.303
		-16.0	1.987	1.836	1.836	2.299	1.405	0.969	-0.063
		-17.0	2.838	2.579	2.579	3.277	1.726	1.290	-0.062
		-18.0	4.643	4.381	4.381	4.631	2.187	1.751	0.001
CSU	13-Nov-13	T	CS-Bio	CS+	CS-	IS-Bio	IS+	IS-	LOG(CS/IS)
		-12.0	0.499	0.682	0.288	0.163	0.075	0.069	0.486
		-13.0	1.010	1.873	0.656	0.330	0.255	0.156	0.486
		-14.0	2.686	4.921	1.737	0.459	0.299	0.200	0.767
		-15.0	6.192	9.914	3.811	1.763	2.587	1.090	0.546
		-16.0	10.297	14.612	6.040	1.953	2.674	1.177	0.722
		-17.0	16.744	23.844	9.837	5.625	4.066	2.569	0.474
		-18.0	27.020	49.350	17.460	9.487	5.346	3.849	0.455
		-19.0	40.174	73.178	25.936	11.494	6.006	4.509	0.543
		-20.0	55.401	116.584	37.555	23.015	10.228	8.731	0.382
CSU	14-Nov-13	T	CS-Bio	CS+	CS-	IS-Bio	IS+	IS-	LOG(CS/IS)
		-18.0	4.175	5.715	2.412	1.490	2.092	0.906	0.447
		-19.0	5.571	9.910	3.566	2.771	2.618	1.433	0.303
		-21.0	12.507	13.803	6.562	8.134	4.437	3.252	0.187
		-22.0	21.512	55.815	15.528	9.997	5.055	3.869	0.333
		-23.0	33.414	64.636	22.027	17.330	7.734	6.548	0.285
		-24.0	64.863	97.105	38.887	26.450	12.001	10.815	0.390
		-25.0	138.913	289.675	93.889	53.411	35.189	23.335	0.415
		-26.0	237.974	579.013	168.656	102.554	51.415	39.561	0.366
		-27.0	347.864	1135.096	266.264	167.467	75.003	63.149	0.317
CSU	14-Nov-13	T	MOUDI-DFT	DFT+	DFT-	IS-Bio	IS+	IS-	LOG(DFT/IS)
		-18.0	0.470	0.269	0.269	1.490	2.092	0.906	-0.501
		-19.0	0.770	0.400	0.400	2.771	2.618	1.433	-0.556
		-20.0	1.300	0.577	0.577	5.233	3.483	2.297	-0.605
		-21.0	2.167	0.786	0.786	8.134	4.437	3.252	-0.574
		-22.0	3.961	1.354	1.354	9.997	5.055	3.869	-0.402
		-23.0	6.533	2.124	2.124	17.330	7.734	6.548	-0.424
		-24.0	11.187	3.750	3.750	26.450	12.001	10.815	-0.374
		-25.0	19.657	7.929	7.929	53.411	35.189	23.335	-0.434
		-26.0	23.834	10.783	10.783	102.554	51.415	39.561	-0.634
-27.0	28.450	11.128	11.128	167.467	75.003	63.149	-0.770		

1335

1340

**Table S3.** Correction factors,  $f_{nu,1mm}$  and  $f_{nu,0.25-0.10mm}$ , applied to MOUDI-DFT samples collected at CSU.  $\mu = N_u(T)/N_o$ , where  $N_u(T)$  is the number of unfrozen droplets at temperature T in the freezing experiment and  $N_o$  is the total number of droplets in the freezing experiment.

MOUDI Stage	$f_{nu,0.25mm-0.1mm}$	$f_{nu,1mm}$ , with uncertainty (+/-)
2	$0.1225\exp(-11\mu) + 1.065\exp(-0.06412\mu)$	0.74, +0.2, -0.13
3	$0.04718\exp(-14.15\mu) + 1.023\exp(-0.02347\mu)$	0.72, +0.8, -0.8 0.65, +0.03, -0.07
4	$0.04252\exp(-13.06\mu) + 1.024\exp(-0.02386\mu)$	1.18, +0.10, -0.15
5	$0.03023\exp(-14.97\mu) + 1.015\exp(-0.01515\mu)$	0.97, +0.03, -0.10
6	$0.5799\exp(-10.57\mu) + 1.148\exp(-0.1408\mu)$	0.75, +0.19, -0.02
7	$0.1151\exp(-10.66\mu) + 1.072\exp(-0.07029\mu)$	0.84, +0.07, -0.11
8	$1.03\exp(-12.79\mu) + 1.268\exp(-0.2422\mu)$	1.01, +0.03, -0.12

1345

**Table S4.** Correction factors,  $f_{nu,1mm}$  and  $f_{nu,0.25-0.10mm}$ , applied to samples collected in Kansas.  $\mu = N_u(T)/N_o$ , where  $N_u(T)$  is the number of unfrozen droplets at temperature T in the freezing experiment and  $N_o$  is the total number of droplets in the freezing experiment.

MOUDI Stage	$f_{nu,0.25mm-0.1mm}$	$f_{nu,1mm}$ with uncertainty (+/-)
2	$0.6505\exp(-7.33\mu) + 1.234\exp(-0.2126\mu)$	3.18, +0.38, -1.03
3	$0.04718\exp(-14.15\mu) + 1.023\exp(-0.02347\mu)$	0.72, +0.8, -0.8 0.65, +0.03, -0.07
4	$0.04252\exp(-13.06\mu) + 1.024\exp(-0.02386\mu)$	1.18, +0.10, -0.15
5	$0.03023\exp(-14.97\mu) + 1.015\exp(-0.01515\mu)$	0.97, +0.03, -0.10
6	$0.5799\exp(-10.57\mu) + 1.148\exp(-0.1408\mu)$	0.75, +0.19, -0.02
7	$0.1151\exp(-10.66\mu) + 1.072\exp(-0.07029\mu)$	0.84, +0.07, -0.11
8	$1.03\exp(-12.79\mu) + 1.268\exp(-0.2422\mu)$	1.01, +0.03, -0.12

**Table S5a:** Correction factors,  $f_{nu,1mm}$  applied to sample M27 (August 17, 2011) collected at the Manitou Experimental Forest Observatory. Only stages overlapping with the CFDC size range were analyzed in this case.

1350

MOUDI Stage	Slide Offset	$f_{nu,1mm}$ lower limit	$f_{nu,1mm}$ upper limit
4	0.5 mm	11.0	29.922
5	0.5 mm	27.304	51.821
6	0.5 mm	5.29	6.273
8	0 mm	1.421	1.829

**Table S5b:** Correction factors,  $f_{nu,1mm}$  applied to sample M28 (August 18, 2011) collected at the Manitou Experimental Forest Observatory. Only stages overlapping with the CFDC size range were analyzed in this case.

MOUDI Stage	Slide Offset	$f_{nu,1mm}$ lower limit	$f_{nu,1mm}$ upper limit
4	1.5 mm	1.217	1.724
5	2 mm	0.73	0.843
6	1.5 mm	1.045	1.167
8	2 mm	0.893	1.077